Atomic Spectroscopy

July/August 2007 Volume 28, No. 4

In This Issue:

Total Urine Arsenic Measurements Using Inductively Coupled Plasma Mass Spectrometry With a Dynamic Reaction Cell

Jeffery M. Jarrett, Robert L. Jones, Kathleen L. Caldwell, and Carl P. Verdon 113

Methodologies for the Determination of Low Concentrations of Lanthanides in Biological Samples by ICP-MS

A.K. Malik, D. Pozebon, V.L. Dressler, M. Zoriy, and J.S. Becker 123

Influence of Organic and Inorganic Acids Commonly Used in Soil Extraction and Digestion Procedures in the Determination of Elements by Inductively Coupled Plasma Optical Emission Spectrometry

Ana Paula Packer and Maria Emília Mattiazzo 129

Aqueous and Acidified Slurry Sampling Approaches in the As, Sb, and Sn Determination of Urban Dust Samples by HG-ETAAS

Jorge Moreda-Piñeiro, Carmen Moscoso-Pérez, María Piñeiro-Iglesias, Purificación López-Mahía 137

Antimony Determination in Mussel Samples by Atomic Absorption Spectrometry Using Palladium-Magnesium Nitrate as Chemical Modifier

B. Curros-Gontad, M.C. Barciela-Alonso, M.D. Buján-Villar, E.M. Peña-Vázquez, and P. Bermejo-Barrera 144

Preconcentration of Nickel in Multi-walled Carbon Nanotubes Pretreated With Potassium Permanganate for Use as Solid-phase Extraction Adsorbent and Determination by Flame Atomic Absorption Spectrometry

Qingxiang Zhou, Huahua Bai, and Junping Xiao 150

ASPND7 28(4) 113–156 (2007)
ISSN 0195-5373

Issues also available electronically.

(see inside front cover)

Atomic Spectroscopy
Vol. 28(4) July/August 2007

Printed in the United States and published six times a year by:

PerkinElmer Life and Analytical Sciences
710 Bridgeport Avenue
Shelton, CT 06484-4794 USA
http://www.perkinelmer.com

SUBSCRIPTION INFORMATION
Atomic Spectroscopy
P.O. Box 3674
Barrington, IL 60011 USA
Fax: +1 (847) 304-6865
E-mail: atsponline@yahoo.com

2008 Subscription Rates
- U.S. $70.00 includes first-class mail delivery worldwide
  $20.00 extra for electronic file.
- Payment by check (drawn on U.S. bank in U.S. funds) made out to: "*Atomic Spectroscopy*"

Electronic File
Send request via e-mail to:
atsponline@yahoo.com

Back Issues/Claims
- Single back issues are available at $15.00 each.
- Subscriber claims for missing back issues will be honored at no charge within 90 days of issue mailing date.

Address Changes to:
Atomic Spectroscopy
P.O. Box 3674
Barrington, IL 60011 USA

Microfilm
Atomic Spectroscopy issues are available from:
University Microfilms International
300 N. Zeeb Road
Ann Arbor, MI 48106 USA
Tel: (800) 521-0600 (within the U.S.)
+1 (313) 761-4700 (internationally)

Guidelines for Authors

Atomic Spectroscopy serves as a medium for the dissemination of general information together with new applications and analytical data in atomic absorption spectrometry.

The pages of *Atomic Spectroscopy* are open to all workers in the field of atomic spectroscopy. There is no charge for publication of a manuscript.

The journal has around 1500 subscribers on a worldwide basis, and its success can be attributed to the excellent contributions of its authors as well as the technical guidance of its reviewers and the Technical Editors.

The original of the manuscript can be mailed to the editor in hard copy including electronic file on disk or CD (or simply by e-mail) in the following manner:

1. If mailed, provide text (double-spaced) and tables in hard copy plus on disk or CD with text and tables in .doc file; figures in doc or tif files.
3. Number the references in the order they are cited in the text.
5. Consult a current copy of *Atomic Spectroscopy* for format.
6. Editor's e-mail:
anneliese.lust@perkinelmer.com

All manuscripts are sent to two reviewers. If there is disagreement, a third reviewer is consulted.

Minor changes in style are made in-house and submitted to the author for approval.

If a revision of the manuscript is required before publication can be considered, the paper is returned to the author(s) with the reviewers' comments.

In the interest of speed of publication, a pdf file of the typeset text is e-mailed to the corresponding author before publication for final approval.

Once the issue has been printed, each author receives a final pdf file of the article including 50 complimentary copies of the article and several copies of the complete issue.

Additional reprints can be purchased, but the request must be made before printing.

PerkinElmer. Inc., holds copyright to all material published in *Atomic Spectroscopy* unless otherwise noted on the first page of the article.

Anneliese Lust
Editor, *Atomic Spectroscopy*
PerkinElmer
Life and Analytical Sciences
710 Bridgeport Avenue
Shelton, CT 06484-4794 USA

Total Urine Arsenic Measurements Using Inductively Coupled Plasma Mass Spectrometry With a Dynamic Reaction Cell

***Jeffery M. Jarrett, Robert L. Jones, Kathleen L. Caldwell, and Carl P. Verdon**
National Center for Environmental Health, Centers for Disease Control and Prevention
4770 Buford Highway NE, Mail Stop F18
Atlanta, GA 30341 USA

ABSTRACT

We describe here a simple, accurate, and rapid method to assess arsenic exposure by analyzing urine with inductively coupled plasma dynamic reaction cell mass spectrometry (ICP-DRC-MS). A comparison of the effectiveness of different reaction gases and internal standards, and results from an interlaboratory comparison of this method with other laboratory methodologies, is presented. Application of this method to biomonitoring for human exposure assessments, epidemiological investigations, and health effect outcome studies is also discussed.

INTRODUCTION

Interest in the level of human exposure to arsenic in the environment and the impact of this exposure has increased as evidence linking chronic low-level exposure to health risks has grown stronger (1), large-scale arsenic poisoning from natural and man-made sources are observed in various countries (2), and as the potential risks to public health from human releases of arsenic-related chemicals into the environment is considered.

Drinking water is an important source of exposure to naturally occurring arsenic (3). Arsenic in natural water sources, predominantly the inorganic forms, occurs largely from minerals dissolving from weathered rocks and soils. In 2000, the U.S. Environmental Protection Agency (EPA) estimated the percentage of U.S. water systems providing water containing more than 5 µg/L arsenic was approximately 12% for groundwater systems and approximately 3% for surface water systems (4). However, the total arsenic concentration in some water systems exceeds 50 µg/L, especially in parts of the West, Midwest, and Northeast U.S. These problems are typically greatest for small towns and rural areas serving less than 10,000 persons which rely more on groundwater for drinking water sources (5). In 2001, the EPA adopted a new standard for the level of arsenic permitted in drinking water, lowering it from 50 to 10 µg/L (6). The rule became effective on February 22, 2002, and the date by which public drinking water systems must comply with the new 10 µg/L standard was January 23, 2006.

People may be exposed to large amounts of the lower toxicity, organic forms of arsenic such as arsenobetaine (AB) and arsenocholine (AC) through their diet, especially through eating seafood (7,8). These two forms are believed to be far less toxic due to their rapid clearance through the kidneys as unchanged molecules (3).

Additional exposure to arsenic can occur from the use of arsenical herbicides, fungicides and insecticides; the occasional use of medicinal arsenic-containing drugs; occupational exposure at work sites that use arsenic and its compounds during manufacturing, particularly among copper, zinc, and lead smelters; along with handling, cutting and sanding construction materials that contain arsenic as a preservative, such as pressure-treated wood.

Investigations leading to the change of the drinking water standard stated that more research is needed on the possible associations between arsenic exposure and public health risks (1). This requires measurements of body fluids that reflect rates of exposure and body burden of this element. Humans eliminate the majority of ingested arsenic through urinary excretion, making urine the biological matrix of choice for the determination of arsenic exposure (9). It is well known that the inorganic species of arsenic are more toxic than the organic forms (3,10). For that reason an approach is also being implemented in our labs where the individual chemical species of arsenic in urine are quantified (11). The total arsenic approach described here, however, allows for a more rapid screening of urine specimens from people possibly exposed to arsenic or to evaluate total environmental exposures to arsenic. Both the total and speciated arsenic approaches will be used to study health effects of arsenic exposure in the U.S. population as part of the National Health and Nutrition Examination Survey (NHANES) survey and to be published in future National Reports on Human Exposure to Environmental Chemicals produced by the Centers for Disease Control and Prevention (CDC) (12). This NHANES survey work will provide urine arsenic data for the U.S. population both before and after the date when public drinking water systems in the U.S. must comply to the new drinking water standards.

**Corresponding author.*
E-mail: JJarrett@CDC.GOV

Since the toxic nature of arsenic has long been recognized, many analytical methods have been used for the determination of arsenic in biological samples (13). Our laboratory measured urine total arsenic for many years with a well-established graphite furnace atomic absorption spectroscopy (GFAAS) method (14). However, as principally a single-element method, GFAAS methods are not conducive to large-scale population surveys where many elements of interest are pursued, such as our participation in the NHANES survey. Due to this limitation, our laboratory has been increasing the use of inductively coupled plasma mass spectrometry (ICP-MS) to perform multi-element analysis of biological samples. Despite the many benefits of ICP-MS for biomonitoring including its multi-element nature, high sensitivity, low limits of detection, and wide linear dynamic range, its applicability to urine arsenic analysis has been historically limited due to polyatomic interferences ($^{40}Ar^{35}Cl^{+}$, $^{40}Ca^{35}Cl^{+}$) on the only natural isotope for arsenic (m/z 75) originating from the argon of the ICP-MS plasma and the chloride and calcium content of the biological samples (15).

There have been many approaches to reduce the effect of these interferences on arsenic determination by ICP-MS, including modification of the plasma by the addition of molecular gases (16,17), mathematical correction based on measurement of related molecular species (17–19), chromatographic separation of the matrix from arsenic (20), physical resolution of the overlapping spectral peaks using sector field ICP-MS (SF-ICP-MS) (21), and chemical resolution of the overlapping ions using inductively coupled plasma dynamic reaction cell™ mass spectrometry (ICP-DRC™-MS) (22,23).

The approach used in our laboratory for the past five years uses ICP-DRC-MS technology. In general, the dynamic reaction cell is pressurized with an appropriate gas and elimination or reduction of argon-based polyatomic interferences takes place through the interaction of the reaction gas with the interfering polyatomic species in the incoming ion beam. The quadrupole in the DRC allows elimination of unwanted reaction by-products that could otherwise react to form new interferences. In the method described here, arsenic (^{75}As) and gallium (^{71}Ga) are measured in simple dilutions of urine by ICP-DRC-MS using argon/hydrogen (90%/10%, respectively) as the cell gas. This single-element ICP-DRC-MS method was developed to be combined with our existing ICP-MS urine multi-element method (24) to form a single method using both standard and dynamic reaction cell modes of the instrument within one analysis.

Method validation included the comparison of this ICP-DRC-MS method with existing, proven methods from labs outside of the Centers for Disease Control and Prevention (GFAAS with Zeeman background correction and ICP-MS analysis with a mathematical correction equation for the $^{40}Ar^{35}Cl$ overlap at m/z 75).

EXPERIMENTAL

Instrumentation

The instrumentation used for these experiments was an ELAN® DRC^{Plus} or ELAN® DRC™ II ICP-MS (PerkinElmer SCIEX, Concord, Ontario, Canada), equipped with a Meinhard quartz nebulizer (Type TQ-30-A3), a DRC quartz cyclonic spray chamber, a 2.0-mm I.D. quartz injector, and nickel sampler and skimmer cones. The original plastic tubing in the instrument which delivers the DRC cell gas from the cylinder, through the instrument to the reaction cell, was replaced with 1/8" stainless steel tubing to eliminate any semi-permeability characteristics which could lead to diffusion of gases through the tubing walls and result in inconsistent performance. Instrumental parameters used are presented in Table I. Cell gas flow rate and RPq parameters were optimized for each instrument. Periodic re-optimization (every 6–12 months) found the cell gas flow rate to change slightly over time for individual instruments. We attribute this to drift over time to calibration of the mass flow controllers.

Materials and Reagents

Water was deionized to ≥18 MΩ.cm using a NANOpure® Diamond™ UV water purification system (Barnstead International, Dubuque, IA, USA). Concentrated nitric acid (Veritas™ double distilled, GFS Chemicals, Columbus, OH, USA), concentrated hydrochloric acid (Veritas™ double distilled, GFS Chemicals, Columbus, OH, USA), and Triton® X-100 (Mallinckrodt Baker, Inc., Phillipsburg, NJ, USA) were used. All elemental standards were from sources (High-Purity Standards, Charleston, SC, USA; SPEX CertiPrep, Metuchen, NJ, USA) traceable to the National Institute for Standards and Technology (NIST, Gaithersburg, MD, USA). A gas mixture of 90% argon (research grade, 99.9997% initial purity, Airgas, Radnor, PA, USA) and 10% hydrogen (research grade, 99.9999% initial purity, Airgas, Radnor, PA, USA) was used as the cell gas for the DRC.

Sample Preparation

Sample preparation for urine specimens was performed by a simple dilution of 0.25 mL urine with 2.25 mL of diluent (2% v/v nitric acid and 10 µg/L gallium internal standard). Matrix-matched calibrators were prepared by adding

TABLE I
Instrumental Parameters

RF Power	1450 W
Gas Flow Rates (Argon)	
Plasma / Auxiliary / Nebulizer	15 / 1.2 / ~0.9 – 1 L/min
DRC Cell Gas	10% H_2 (99.9999% purity)
	90% Ar (99.9997% purity)
	0.2 – 0.6 sccm
	(optimized for elimination of ArCl)
Sample Uptake Rate	~ 0.65 mL/min
Rinse	90 s at ~1.3 mL/min using
	5% (v/v) nitric acid,
	0.002% Triton® X-100
RPQ	0.65 – 0.75
Ion Lens Voltages	AutoLens™
Detector Mode	Pulse
Sweeps / Reading	20
Readings / Replicate	1
Replicates	3
Dwell Time	50 ms
Blank Subtraction	After Internal Standard
Curve Type	Simple Linear (calibrated to 300 µg/L)

0.1 mL of a calibration standard into 0.9 mL of pooled urine (tested to be < 5 µg/L As) and 9 mL of diluent. Sample dilutions were accomplished using a Micromedic Digiflex™ automatic pipette (Titertek, Huntsville, AL, USA).

Methods of the Interlaboratory Comparison

Method validation included an inter-laboratory comparison with two external laboratories. Lab 1 used graphite furnace atomic absorption spectroscopy with Zeeman background correction (GFAAS). Arsenic in urine was digested and oxidized to the pentavalent form. The arsenic was converted to the iodide and extracted into toluene. The arsenic complex was then back-extracted into an acidic nickel nitrate solution and quantitated by GFAAS. Lab 2 used ICP-MS and corrected for the chloride interferences mathematically ($I_{75} = I_{75} - 0.00002^* I_{35}$). Urine was diluted 1:20 with 0.5% (v/v) nitric acid. Internal standard (Y) and ethanol were spiked into the dilution (50 µL of 2 mg/L Y and 100 µL of ethanol, respectively), then analyzed by ICP-MS using matrix-matched external calibration.

RESULTS AND DISCUSSION

Selection of Internal Standard

Isotope ^{71}Ga was selected as the internal standard after testing ^{74}Ge and ^{126}Te. Isotope ^{69}Ga was not used for gallium due to potential interference from $^{138}Ba^{++}$. Brief tests using ^{74}Ge yielded comparable results; however, the potential for interference from ^{74}GeH at m/z 75 discouraged its use. In tests comparing gallium and tellurium as internal standards for arsenic, 41 different urine materials with a range of arsenic concentrations (15–530 µg/L) were analyzed in 3–13 runs. The between-run reproducibility when using ^{126}Te as the internal standard (average 8.5% RSD) was generally inferior to that observed when using gallium (average 4.9% RSD).

Selection of Reaction Cell Gas

The use of ICP-DRC-MS with hydrogen in argon as a reaction gas for the elimination of the $ArCl^+$ interference at m/z 75 has been described previously (23,25–28). These publications indicate that the hydrogen component of the cell gas mixture reacts with the $ArCl^+$ interference to eliminate the $ArCl^+$ interference at m/z 75. Figure 1 shows the results of total arsenic analysis using different proportions of hydrogen in argon as the reaction cell gas. The urine reference materials analyzed were spiked with Cl^- (>400 mM Cl^-) to simulate approximately twice the highest expected adult urine chloride concentrations (29). The results matched target values best when using either pure argon or a mixture of 10% hydrogen in argon as the reaction cell gas. The largest bias was observed when using 50% hydrogen in argon. These data suggested that the underlying mechanism for removal of the $ArCl^+$ interference was possibly disassociation of the polyatomic ion after collision with argon atoms in the cell. In light of the uncertainty of mechanism and suggestions from the ICP-DRC-MS manufacturer, the 10% hydrogen and 90% argon gas mixture was selected as the reaction cell gas for the method. The use of pure argon may be investigated further in future biomonitoring work since it would be logistically simpler with argon gas already available in the laboratory for the operation of the instrument.

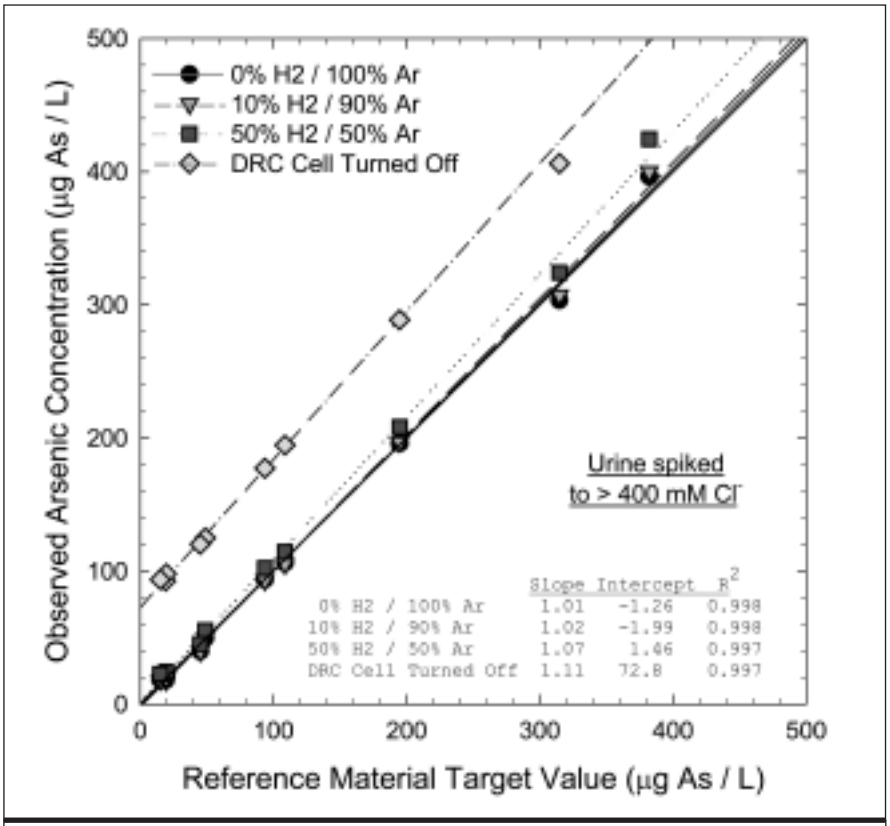

Fig. 1. Selection of cell gas.

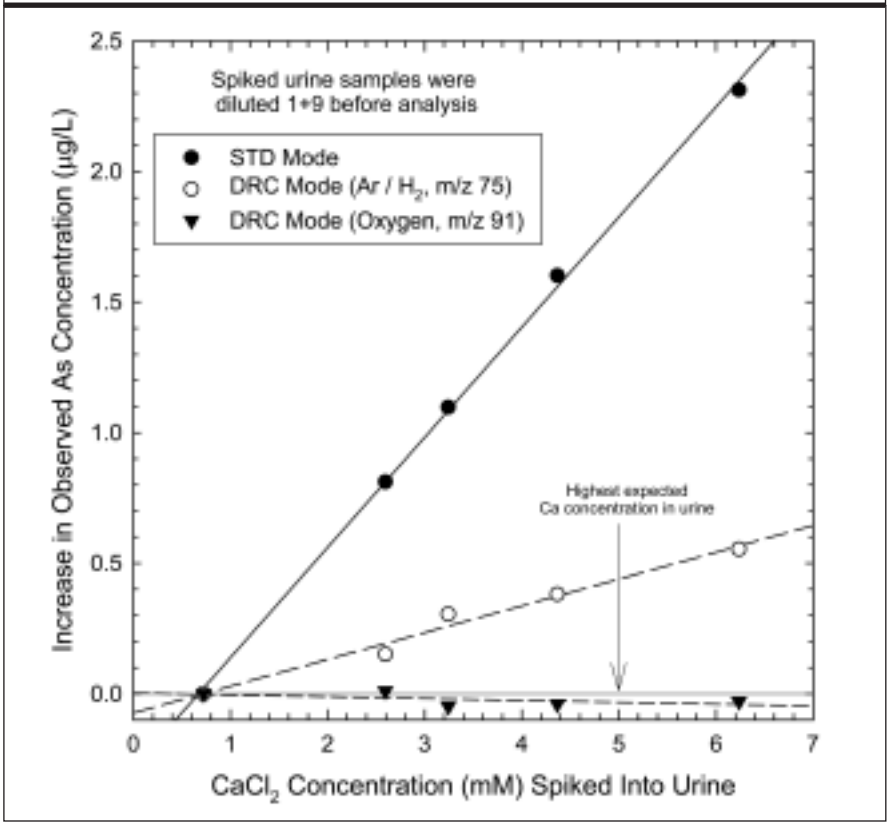

Fig. 2. Effect of Ca and Cl interferences on As measurement.

An alternative to removing the interferences from m/z 75 is to use oxygen as the reaction gas and monitor m/z 91 for $^{75}As^{16}O^{+}$ (23,30,31). While the use of Ar / H_2 as a DRC gas serves well to eliminate the $^{40}Ar^{35}Cl^{+}$ interference observed from a chloride-containing matrix (see Figure 1), a small interference (approximately 0.4 µg/L) remains at m/z 75 when the matrix contains both high chloride and high calcium levels (see Figure 2). Mass spectrum scans of solutions containing calcium or calcium and chloride matrices suggest that the interference is mainly a result of $^{40}Ca^{35}Cl^{+}$, but also of a calcium hydroxide species [possibly $CaO\cdot(H_3O)^{+}$]. In all of these experiments, the concentration of calcium was equal to the highest expected in urine (29), and the concentration of chloride was double the molar concentration of calcium. It can be seen in Figure 2 that we found the use of oxygen as the reaction cell gas (0.32 sccm cell gas flow rate, RPq = 0.7) was effective at avoiding all interferences being observed at m/z 75 in high chloride and calcium matrices. We investigated the possibility of interference from zirconium at m/z 91, but found that zirconium reacts quickly in the presence of the oxygen reaction cell gas to form ZrO and ZrO_2 so that it would not interfere with measurements of $^{75}As^{16}O^{+}$ at m/z 91. This reaction has been reported on elsewhere (32,33).

TABLE II
Comparison of Precision for Urine Arsenic Analysis
(All units µg/L As.)

Sample ID	Target	N	SD (m/z 75) H_2	SD (m/z 91) O_2
S-03-16	30.0	3	1.2	2.3
S-03-15	42.7	4	1.4	2.2
S-03-09	97.4	4	2.6	4.5
S-03-10	145.3	4	3.9	6.6
S-03-05	155.1	4	3.5	6.6
S-03-12	271.2	4	5.6	9.3
S-03-08	292.2	4	7.2	11.4

Arsenic results were obtained by running multiple DRC modes simultaneously. Monitoring of ^{75}As was done while using a 90% argon, 10% hydrogen DRC gas setup on channel A (0.6 sccm, RPq 0.65). $^{75}As^{16}O$ was monitored at m/z 91 while using a 100% oxygen DRC gas setup on channel B (0.32 sccm, RPq 0.7).

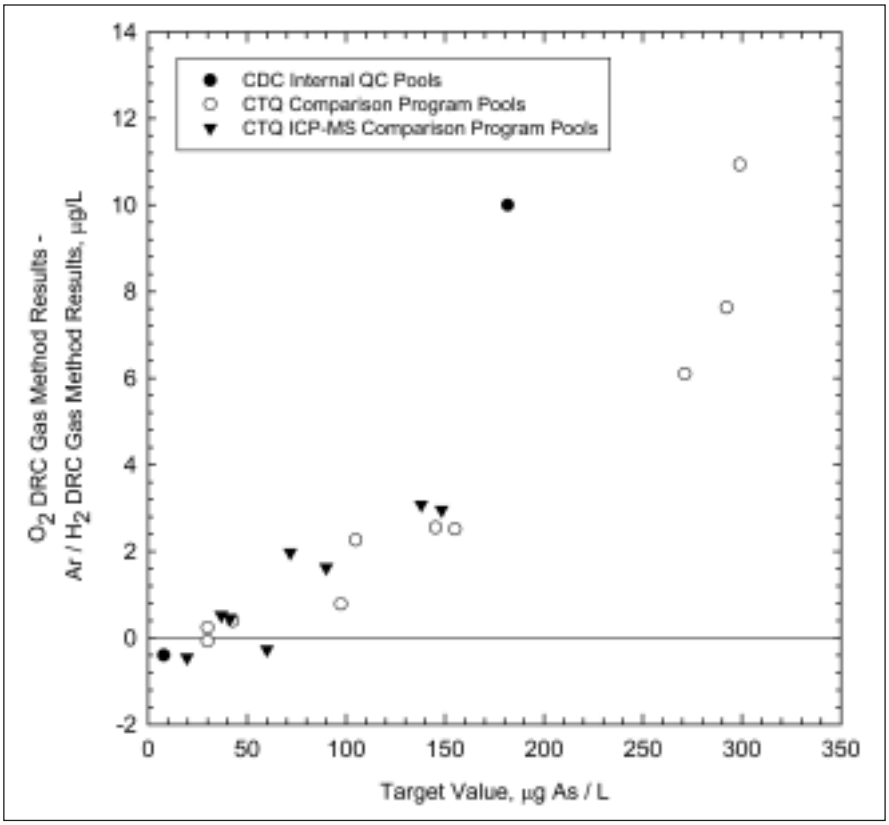

Fig. 3. Comparison of urine arsenic concentration results obtained using a DRC gas of 90% argon, 10% hydrogen, monitoring ^{75}As at m/z 75 with results obtained using a DRC gas of 100% oxygen, monitoring $^{75}As^{16}O$ at m/z 91. The difference between the results of the two methods shows the positive bias of the oxygen method relative to the argon / hydrogen method.

Urine arsenic results from the oxygen reaction-gas method, however, had a higher between-run variability (see Table II) and a positive bias (see Figure 3) relative to the Ar / H_2 DRC gas method. We decided that the relatively small interferences possible when using an argon / hydrogen reaction gas would be preferable to the higher uncertainty and bias of the oxygen reaction gas method.

Matrix Effects of Carbon on Arsenic Signal

Matrix-induced signal enhancement in ICP-MS analysis from carbon on arsenic has been previously reported in the literature (17,34). Based on these reports, we tested the addition of alcohol to the diluent to enhance the arsenic signal. The addition of 2-3% methanol or 1–2% ethanol to the diluent enhanced the arsenic signal by a factor of 3–4. However, the standard deviation of individual concentration measurements was 2–5 times higher when alcohol was added to the diluent. Between-run precision was not affected by the addition of alcohol. Due to the effects on measurement precision, we do not add alcohol to the diluent.

Due to the matrix-induced signal enhancement from carbon on arsenic, performing a larger dilution on a patient urine sample than is performed on the matrix of the calibrators will result in a lower observed arsenic concentration for the patient urine sample. For this reason, validating concentration measurements above the typical calibration concentration range is not performed by extra dilutions to the patient urine samples. Instead, due to the large linear dynamic range of ICP-MS, additional calibrators are used to verify calibration linearity above the typical calibration range. We have verified this range to greater than 6000 µg/L.

DRC Stabilization Time

Signal drift is typically observed when beginning the DRC method which is not identical for both the analyte and the internal standard. For this reason, the instrument is operated in DRC mode for at least 45–60 minutes prior to beginning the analysis to reach the best signal ratio stability (^{75}As / ^{71}Ga). Typical operating procedure for daily analysis includes plasma ignition, instrument performance check in standard mode after 45 minutes, purge of the tubing leading to the mass flow controllers for 1 minute, and analysis of a urine standard repeatedly in DRC mode for at least 1 hour. The stability of the ^{75}As / ^{71}Ga ratio from the urine standard analyses is checked using a Microsoft® Excel® template and the analytical run is started if drifting of the signal ratio has stopped. Out of 78 runs, 23% required no stabilization time, 52% of the runs reached acceptable ratio stability within 30 minutes, 8% required 1 hour, 9% required 1–2 hours, and 8% required greater than 2 hours. There are no apparent associations between system maintenance and time required to reach acceptable ratio stability. The magnitude of the drift during the stabilization time was generally within 10% of the target arsenic concentration (85% of runs), but in some cases was as high as 40%. Drift for both ^{75}As and ^{71}Ga during the stabilization time was almost always in the positive direction, and the increase for ^{75}As was typically greater. Operating the ICP-DRC-MS in DRC mode for one or more hours before analysis without repeatedly analyzing a diluted urine matrix does not eliminate drift of the observed arsenic concentration; however, it reduces the number of urine matrix sample measurements which need to be made in the stabilization time. From 49 experiments where this was done, we found that 55% of runs required no additional stabilization time, 31% of runs reached acceptable stability within 30 minutes, 6% required 1 hour, 6% required 1-2 hours, and 2% required greater than 2 hours. The issues related to signal drift observed here were specific to DRC mode operation of the instruments; no drift issues like this were observed when the instrument was operated in the Standard mode of operation. We have observed similar issues with drift when using the DRC for mixed-mode analysis where the method contains both a DRC mode component (cell is pressurized) and a standard mode component (cell is not pressurized). It is thought that the problem is related to impurities within the cell gas introduction system which can require an extended time to flush out. After stabilization time, drift in the observed arsenic concentration over the first 8 hours of analysis is approximately 3 ± 4%. Recalibration is performed after approximately 8 hours of analysis.

Atomic Spectroscopy
Vol. 28(4), July/August 2007

TABLE III
Results for Analysis of NIST Reference Materials and CDC Bench QC (µg/L As)

	Target Value ± 1SD	Observed Value ± 1SD	N
NIST SRM 2670 Normal	(60, info. value)	79.7 ± 3.5	89
NIST SRM 2670 Elevated	480 ± 100	533.3 ± 28.3	32
NIST 2670A Low	(3, info. value)	2.6 ± 0.3	9
NIST 2670A High	No value given	215.0 ± 5.2	9
NH0119	–	8.2 ± 0.8	194
NH0120	–	179.7 ± 5.4	195

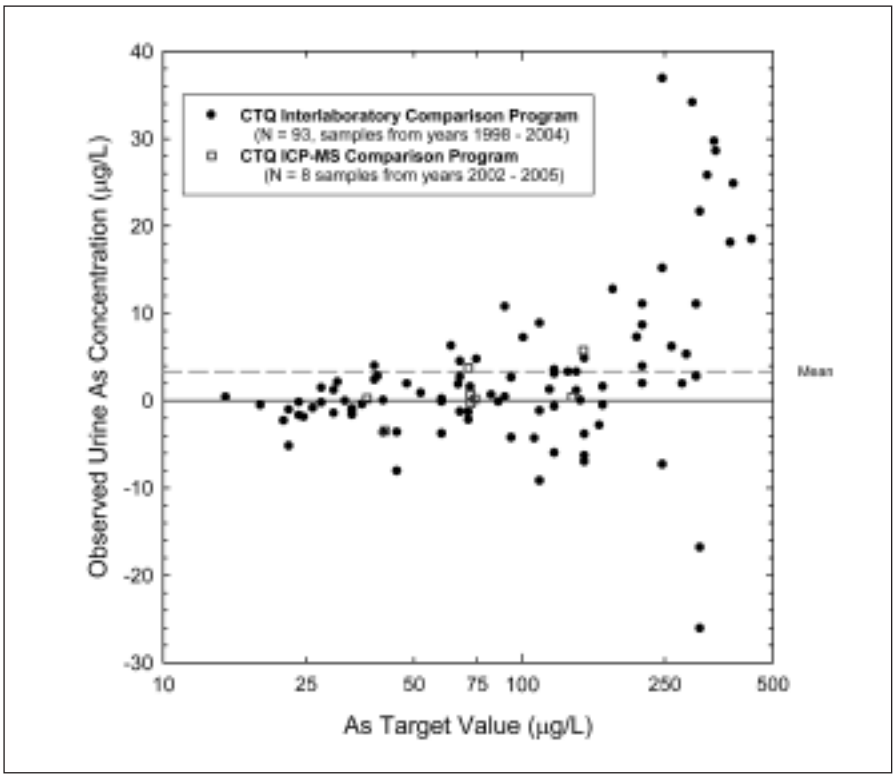

Fig. 4. Analysis of reference materials from the Center for Toxicology of Quebec (CTQ).

Accuracy

Table III presents the observed and informational or certified values for urine standard reference materials (SRM) from NIST. Observed concentrations are in agreement with the limited NIST values which are available. Due to the limited certified target values for the NIST reference materials, urine reference materials from the Centre de Toxicology du Quebec (Quebec, Canada) were also used in validating the accuracy of the method (see Figure 4, slope = 1.047, intercept = –3.188, $r^2 = 0.995$, N = 101). All observed results for the Centre de Toxicology du Quebec (CTQ) reference materials were within two standard deviations of the target values assigned for the comparison programs.

Precision

The between-run precision of urine total arsenic measurements for low and high concentration bench quality control pools is shown in Figures 5 and 6. The coefficient of variation for measurements of the two pools collected over a 33-month period in 192 runs was 9.8% and 3.0% for the low and high pools respectively. Each pool is measured both at the beginning and at the end of the run and quality control decisions for each run are made considering the average of both measurements, the range of the duplicate measurements, and trends of the averages across multiple runs.

Effect of Chloride Concentration

The effect of chloride concentration in the urine sample on the observed total arsenic concentration (as $^{40}Ar^{35}Cl^+$ and $^{40}Ca^{35}Cl^+$) was evaluated as part of an interlaboratory comparison with two laboratories (see Table IV). Chloride spiked to the highest expected physiological levels had little to no impact on observed total arsenic concentrations from any of the methods participating in the interlaboratory comparison. The calcium content of the urine samples was unknown. No effect is expected on GFAAS results since that measurement technique is not affected by chloride interferences.

The ICP-MS method using the $I_{75} = I_{75} - 0.00002 * I_{35}$ correction equation performed well at the elimination of the chloride interferences. To accomplish this, however, the analyst determines the correct coefficient for the I_{35} correction term at least daily to determine the I_{75} / I_{35} relationship which is controlled by plasma conditions. The ICP-DRC-MS results reflect a comparable elimination of effect from chloride without the necessity for daily verification or adjustment of the correction equation.

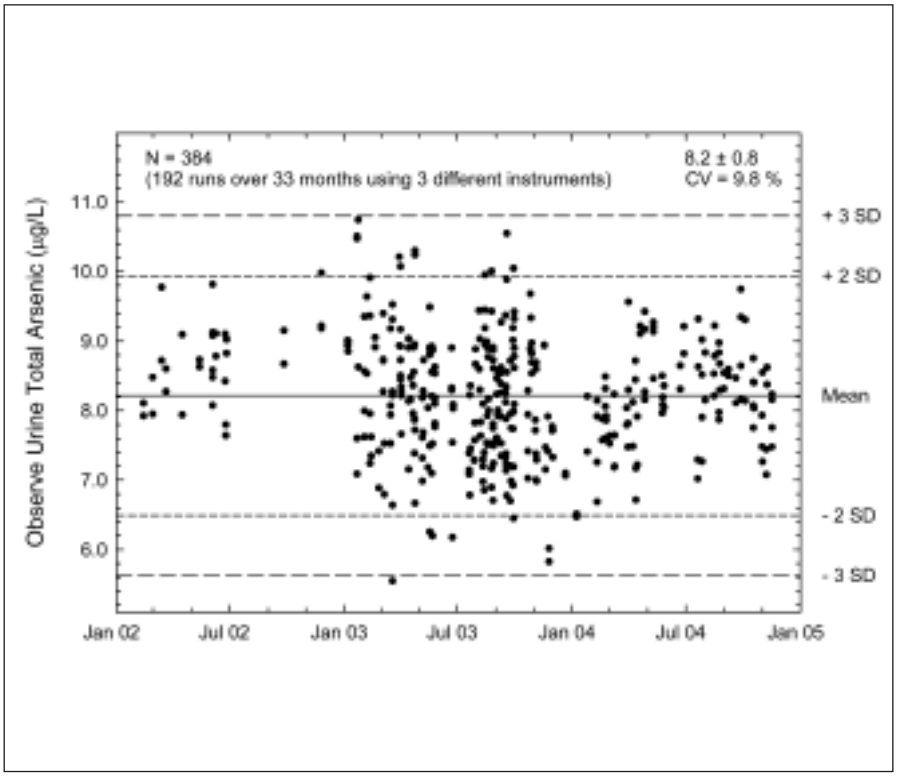

Fig. 5. Analysis of low "bench" (internal) quality control material.

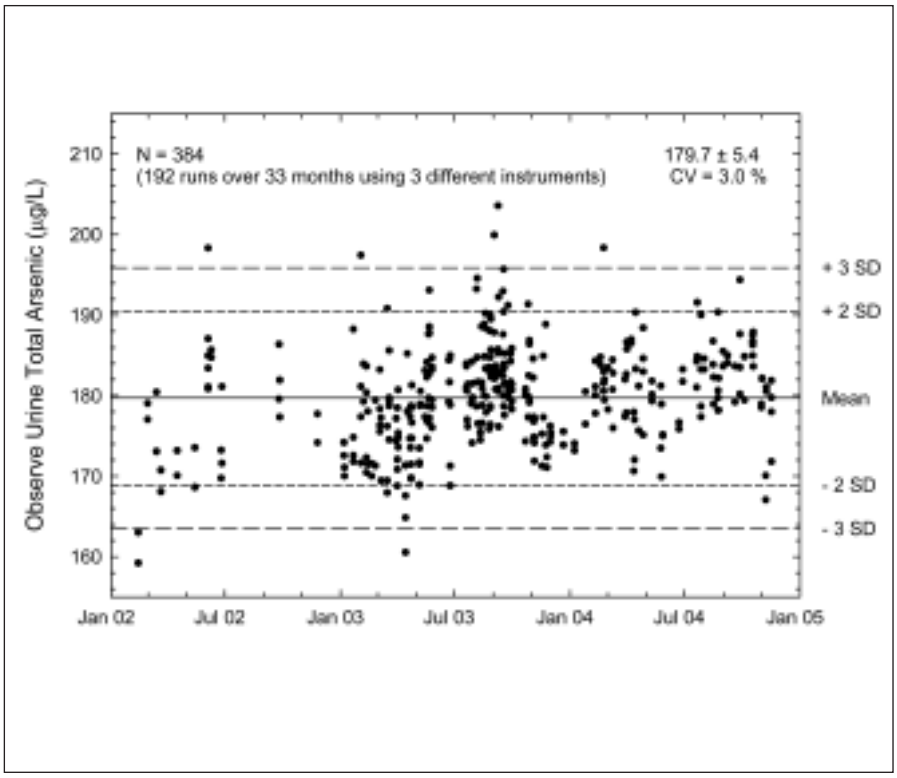

Fig. 6. Analysis of high "bench" (internal) quality control material.

Spike Recovery

Spike recoveries were also tested as part of the interlaboratory comparison (see Table V). Recoveries observed were 81–103% for the ICP-DRC-MS method, 63–100% for the ICP-MS method, and 87–200% for the GFAAS method. All methods reported lower recovery (81–87%) for the 30 µg/L spiked sample. The 200% recovery observed by the GFAAS method for the 5 µg/L spike could have been due to being close to the limit of detection (limit of detection value unknown).

CONCLUSION

The ICP-DRC-MS method presented here successfully eliminates the $^{40}Ar^{35}Cl^{+}$ interference typically experienced in urine total arsenic analysis by ICP-MS without the need for correction equations that must be updated daily to reflect instrument conditions. The remaining interference from $^{40}Ca^{35}Cl^{+}$ is minimal, and preferable to the larger between-run uncertainty observed when using oxygen as a reaction gas and monitoring $^{75}As^{16}O^{+}$. The accuracy and precision of the method has been shown to be acceptable for the routine biomonitoring of urine samples and capable of being maintained over multiple years of operation. While the analysis of urine samples for total arsenic does not provide important information regarding the species of the arsenic, it allows a rapid determination of the overall exposure to arsenic species and can be used to determine the priority of speciation analysis which may need to be performed subsequently. The method is applicable to a wide range of urine arsenic concentrations and is therefore useful for biomonitoring persons with a wide range of arsenic exposures. One of the applications of this method has been the National Health and Nutrition Examination Survey (NHANES), the results of which will be published in future National Reports to

Table IV
Inter-laboratory Comparison Results:
Effect of Chloride on Observed Arsenic Concentration
(observed bias, %)

Method	50 mM Cl^-	200 mM Cl^-
ICP-DRC-MS (CDC)	–0.3 ± 1.1 %	0.9 ± 4.7 %
GFAAS (Lab 1)	0.5 ± 14.3 %	–6.6 ± 4.3 %
ICP-MS with mathematical correction equation (Lab 2)	–2.3 ± 5.2 %	0.4 ± 1.0 %

TABLE V
Inter-laboratory Comparison Results: Spike Recovery (%)

Sample Spike Conc. (µg/L As)	ICP-DRC-MS (CDC)	ICP-MS With Correction Equation	GFAAS
5	99%	100%	200%
30	81%	80%	87%
60	90%	90%	98%
90	103%	99%	107%
150	96%	63%	94%
190	98%	92%	95%
380	97%	92%	101%
550	98%	94%	91%
2000	97%	90%	88%

the Exposure of Environmental Chemicals (35). Future work will make use of the multi-element nature of the ICP-DRC-MS technology to combine this method with other similar ICP-MS and ICP-DRC-MS urine analysis methods in our laboratory. This will permit the more efficient measurement of multiple elements within one sample analysis.

Received April 16, 2007.

REFERENCES

1. National Research Council. Subcommittee to Update the 1999 Arsenic in Drinking Water Report. Committee on Toxicology. Board on Environmental Studies and Toxicology, Arsenic in Drinking Water: 2001 Update. 2001, Washington, D.C.: National Academy Press. 244.
2. D.K. Nordstrom, Science 296 (5576), 2143 (2002).
3. Agency for Toxic Substances and Disease Registry (ATSDR), (DRAFT) Toxicological profile for arsenic. Atlanta, GA: U.S. Department of Health and Human Services, Public Health Service (2005).
4. U.S. Environmental Protection Agency, Arsenic Occurrence in Public Drinking Water Supplies. Washington, D.C. (2000).
5. M. Tiemann, Arsenic in Drinking Water: Recent Regulatory Developments and Issues. Library of Congress. Congressional Research Service (2001).
6. U.S. Environmental Protection Agency, National Primary Drinking Water Regulations; Arsenic and Clarifications to Compliance and New Source Contaminants Monitoring. Final Rule. pp. 6976-7066 (Jan 22, 2001).
7. J.F. Lawrence, J.F., et al., J. Agric. and Food Chem. 34(2), 315 (1986).
8. R.W. Dabeka, et al., J AOAC Int. 76(1), 14 (1993).
9. National Research Council Subcommittee on Arsenic in Drinking Water, Arsenic in drinking water. Washington, D.C.: National Academy Press. 310 (1999).
10. R.S. Oremland and J.F. Stolz, Science 300(5621), 939 (2003).
11. C. Verdon, K.L. Caldwell, and R.L. Jones, Urine Arsenic Speciation by High Performance Liquid Chromatography Inductively Coupled Plasma Dynamic Reaction Cell Mass Spectrometry (HPLC-ICP-DRC-MS). Centers for Disease Control and Prevention (2004).
12. Department of Health and Human Services. Centers for Disease Control and Prevention, Candidate Chemicals for Possible Inclusion in Future Releases of the National Report on Human Exposure to Environmental Chemicals. pp. 56296-56298 (Sep. 30, 2003).
13. R. Iffland, Arsenic, in Handbook on Metals in Clinical and Analytical Chemistry, H.G. Seiler, A. Sigel, and H. Sigel, Editors. Marcel Dekker, Inc.: New York. pp. 237-253 (1994).
14. D.C. Paschal, M.M. Kimberly, and G.G. Bailey, Anal. Chim. Acta 181, 179 (1986).
15. S.H. Tan and G. Horlick, Appl. Spectrosc. 40(4), 445 (1986).
16. J.S. Wang, E.H. Evans, and J.A. Caruso, J. Anal. At. Spectrom. 7(6), 929 (1992).
17. C.J. Amarasiriwardena, Analyst 123(3), 441 (1998).
18. D.E. Nixon and T.P. Moyer, Spectrochim. Acta Part B - Atomic Spectroscopy, 51(1), 13 (1996).
19. M.M. Kershisnik, Clin. Chem. 38(11), 2197 (1992).

20. C. B'Hymer and J.A. Caruso, J. Chromatogr. A, 1045(1-2), 1 (2004).

21. M.J. Campbell, C. Demesmay, and M. Olle, J. Anal. At. Spectrom. 9(12), 1379 (1994).

22. J.M. Jarrett, et al., FP5: Investigations into Urine Arsenic Analysis by ICP-DRC-MS. in Winter Conference of Plasma Spectrochemistry. Scottsdale, Arizona: ICP Information Newsletter (2002).

23. D.E. Nixon, et al., Spectrochim. Acta Part B - Atomic Spectroscopy, 59(9), 1377 (2004).

24. K.L. Caldwell, et al., At. Spectrosc. 26(1), 1 (2005).

25. S.D. Tanner and V.I. Baranov, At. Spectrosc. 20(2), 45 (1999).

26. K. Neubauer and U. Voellkopf, At. Spectrosc. 20(2), 64 (1999).

27. S.D. Tanner, V.I. Baranov, and D.R. Bandura, Spectrochim. Acta Part B-Atomic Spectroscopy, 57(9), 1361 (2002).

28. S.D. Tanner, V.I. Baranov, and U. Voellkopf, J. Anal. At. Spectrom. 15(9), 1261 (2000).

29. Tietz Textbook of Clinical Chemistry. 3rd ed, ed. C.A. Burtis and E.R. Ashwood. Philadelphia, PA: W.B. Saunders Company (1999).

30. W. Reuter, et al., Speciation of Five Arsenic Compounds in Urine by HPLC/ICP-MS. PerkinElmer Application Note D-6736 (2003).

31. K. Kinoshita, O. Shikino, Y. Seto, and T. Kaise, Appl. Organometallic Chem. 20(9), 591 (2006).

32. V.G. Anicich, An index of the literature for biomolecular gas phase cation-molecule reaction kinetics. NASA/Jet Propulsion Laboratory (2003).

33. D.K. Bohme, 2007 (cited 6/13/07); Available from: http://www.chem.yorku.ca/profs/bohme/research/element/Zr.html

34. E.H. Larsen and S. Sturup, J. Anal. At. Spectrom. 9, 1101 (1994).

35. National Center for Environmental Health, Third National Report on Human Exposure to Environmental Chemicals. Department of Health and Human Services, Centers for Disease Control and Prevention: Atlanta, GA, USA. pp. 1–467 (2005).

Methodologies for the Determination of Low Concentrations of Lanthanides in Biological Samples by ICP-MS

A.K. Malik[b], D. Pozebon[c], V.L. Dressler[d], M. Zoriy[a], and *J.S. Becker[a]

[a] Central Division of Analytical Chemistry, Research Centre Jülich, D-52425, Jülich, Germany

[b] Department of Chemistry, Punjabi University, Patiala – 147 002, Punjab, India

[c] Universidade Federal do Rio Grande do Sul, Instituto de Química, 91500-970, Porto Alegre, RS, Brazil

[d] Universidade Federal de Santa Maria, Departamento de Química, 97105-900, Santa Maria, RS, Brazil

ABSTRACT

This work deals with the development of analytical methods for lanthanide determination in biological samples. One method consists of using capillary electrophoresis (CE) for lanthanide separation prior to the detection by inductively coupled plasma mass spectrometry (ICP-MS). The lanthanides are extracted from the sample solution by liquid-liquid extraction with bis(2-ethylhexyl)orthophosphoric acid (HDEHP) in toluene at pH 2.0 and then back-extracted into an aqueous phase using 6 mol L^{-1} HNO_3. After solvent evaporation, the residue is dissolved with water, and 32 nL of this solution injected into the capillary. A mixture of 6 mmol L^{-1} 8-hydroxyisobutyric acid (HIBA) with pH 4.2 is used as the electrolyte solution. It is demonstrated that the lanthanides are separated under this condition. The other method consists of using a micro nebulizer-desolvation system for introducing the sample into the plasma of an ICP-MS. The oxide formation rate is remarkably decreased by using this introduction system, allowing accurate lanthanide determination. The developed methods were applied to the determination of lanthanides at the ng g^{-1} levels in mussel tissue. The concentrations of the elements were below the detection limits of the CE-ICP-MS method, but detected and quantified by using the micro nebulizer-desolvation system.

INTRODUCTION

Lanthanides have been increasingly used in a number of fields, thus spreading their entrance into the environment, animal and human bodies. Therefore, it is important to develop analytical methods for the determination of low concentrations of these elements in biological samples.

Inductively coupled plasma mass spectrometry (ICP-MS) is one of the most suitable techniques for lanthanide determination at low concentrations due to its high sensitivity and relatively good selectivity. However, interferences from isobaric atomic ions and polyatomic ions are found in multi-element ICP-MS determinations. Therefore, for accurate determination of lanthanides by ICP-MS, the possibility of interference from isobaric atomic ions and polyatomic ions needs to be considered. The determination will be more difficult with a high concentration ratio of lighter to heavier lanthanides. Additionally, Ba is usually found in relatively high concentrations in environmental, geological, and biological samples and, therefore, its oxides and hydroxides can interfere with Nd, Sm, Eu, and Gd (1). With a maximum mass resolution of 10,000 for double-focusing ICP mass spectrometers, most isobaric interferences of atomic and oxide ions can be separated. In practice, the theoretically required mass resolution is insufficient if the intensity of oxide ions is significantly higher than that of the analyte ions (2,3). For this reason, other alternatives should be used in order to resolve the isobaric interferences as, for instance, lanthanide separation (4,5) and/or water desolvation-nebulizer systems. In this approach, the water-solvent molecules that enter the plasma can be drastically reduced, therefore, decreasing oxide and hydroxide formation. It has already been observed (6,7) that the formation of B, Cl, K, Ca, Zn, and U oxides were greatly reduced by employing this type of system.

Capillary electrophoresis (CE) is a suitable separation technique in which solvated ions in an electrolyte solution are separated according to their mobilities in solution while subjected to an electrical field. Lanthanides, because they are similar in size and chemical properties, present a challenge for chemical separation. Capillary electrophoresis (CE) is a useful separation technique for lanthanides, which has been demonstrated (4,8,9). By using HIBA (hydroxybutiric acid), each lanthanide was selectively complexed with the separation based on the extent of complexation (8). The major advantages of CE are short separation times (in comparison to liquid chromatography) and requiring reduced amounts of sample, solvents, and chemicals. Furthermore, the good detection capacity of ICP-MS makes it a suitable detector for low concentrations of lanthanides after their separation by CE.

The aim of the present study was to develop analytical methods for

*Corresponding author.
E-mail: s.becker@fz-juelich.de

lanthanide determination at trace levels in biological samples. The use CE-ICP-MS and a micro nebulizer-desolvation system for introducing the sample solution into an ICP-MS were investigated.

EXPERIMENTAL

For all mass spectrometric measurements, a quadrupole-based ICP-MS (ICP-QMS), Model ELAN® 6000 or ELAN® 6100 (PerkinElmer SCIEX, Concord, Ontario, Canada), was used. An APEX (from ESI, Omaha, NE, USA) sample introduction system was used. With this system, the sample is self-aspirated with a PFA microconcentric nebulizer. The aerosol passes through a heated cyclonic spray chamber (140 °C) and is then transported to a Peltier-cooled multi-pass condenser (–5 °C). For lanthanide separation, a Waters Quanta 4000 capillary ion analysis system (Waters Corporation, Boston, MA, USA) was used. A Micromist nebulizer (Model AR40-1F02 from Glass Expansion, Victoria, Australia) attached to a Cinnabar mini cyclonic spray chamber (Glass Expansion) was used for introducing the eluent into the plasma of the ICP-MS. The CE separation conditions are shown in Table I.

All measurements were performed under optimized conditions with respect to gas flow rate, rf power, torch position, and ion lens voltage. Except for ^{141}Pr, ^{159}Tb, and ^{165}Ho, which are monoisotopic, the isotopes free of elemental isobaric interferences and/or most abundant were chosen. The main parameters are summarized in Table II.

CE Conditions and Interface

The schematic representation of the CE interface to ICP-MS is discussed and shown in reference (4). It basically consists of a PEEK tubing, a PEEK finger, and a PEEK four-way tee union (Upchurch Scientific). PEEK tubing (0.50 mm i.d. x 1.6 mm o.d.) was used as a sleeve around the CE capillary into the four way tee union. The makeup electrolyte solution was aspirated through a PTFE tubing (1.00 mm i.d. x 1.6 mm o.d.). A 0.50-mm o.d. Pt interface electrode was sealed through a PEEK sleeve (0.50 mm i.d. x 1.6 mm o.d.) and sealed inside the back of the nebulizer via Tygon® tubing.

Prior to use, all CE solutions were degassed and filtered through a 0.45-mm filter paper. All CE electrolytes were prepared fresh daily. The new capillaries were conditioned using 0.1 mol L^{-1} HCl, 0.1 mol L^{-1} NaOH, and CE electrolyte solution. After each sample run, the capillary was washed with electrolyte solution for 2 min. The usual current across the interface ranged from of 4.5 µA to 9.0 µA. A make-up solution was used for maintaining a stable electrical connection to the detection end of the CE capillary and controlling the laminar flow. The data obtained in the CE-ICP-MS analysis was exported and analyzed as Excel® files.

Chemicals and Sample Preparation

For all solutions and sample preparation, Milli-Q™ water (18.2 MΩ cm) was used. The HNO_3, HCl, and NaOH, and monoelement lanthanide standard solutions were purchased from Merck (Darmstadt, Germany). The electrolyte solution used for CE was 6 mmol L^{-1} hydroxybutiric acid (HIBA) from Fluka, with 5 mmol L^{-1} sodium acetate (CIA-Pak UV Cat 1 from Waters), which was adjusted to pH 4.2 with 0.1 mmol L^{-1} HCl

TABLE I
Capillary Electrophoresis Operating Conditions

Parameter	Condition
Power Supply	+ 25 kV
Capillary	i.d. 75 µm o.d. 365 µm Length = 80 cm
Electrolyte Solution	6 mmol L^{-1} HIBA, 5 mmol L^{-1} sodium acetate/UV Cat–1, pH = 4.3 (in HCl)
ICP-MS Make-up Buffer	0.005% (v/v) HNO_3
Temperature	24 °C
Injection Volume	35 nL (30 s, hydrodynamic)

TABLE II
Instrumental Parameter and Analysis Conditions Used for ICP-QMS Measurements

	Sample Introduction	
	CE–Micromist ELAN 6000	PFA-APEX ELAN 6100
RF Power	1300 W	950 W
Cooling Gas Flow Rate	14 L min^{-1}	14 L min^{-1}
Auxiliary gas flow rate	0.8 L min^{-1}	1.2 L min^{-1}
Nebulizer gas flow rate	0.85 L min^{-1}	0.90 L min^{-1}
Solution uptake rate	200 µL min^{-1}	330 µL min^{-1}
Number of Isotopes per Run	21	14
Scanning Mode	Peak Hopping	Peak Hopping
Sampler and Skimmer Cones	Ni	Ni
Monitored Isotopes	^{139}La, ^{140}Ce, ^{141}Pr, ^{143}Nd, ^{146}Nd, ^{147}Sm, ^{149}Sm, ^{151}Eu, ^{153}Eu, ^{155}Gd, ^{157}Gd, ^{159}Tb, ^{162}Dy, ^{163}Dy, ^{165}Ho, ^{166}Er, ^{167}Er, ^{169}Tm, ^{172}Yb, ^{173}Yb, and ^{175}Lu	

solution. Three 50-mg aliquots of mussel tissue (Certified Reference Material - BCR 668, from the Community Bureau of Reference, Brussels, Belgium) were microwave-digested (Microwave Accelerated Reaction Systems, MARS-5 from CEM Corporation, Mathews, NC, USA) using an oxidizing mixture of 0.8 mL HNO_3 and 0.2 mL H_2O_2. The digestion was carried out with the following heating program: 150 W for 10 min, cooling for 2 min, 300 W for 10 min, and cooling for 30 min. The digested sample was transferred to a disposable plastic tube and made up to 5 mL with water. When the APEX system was used, this solution was analyzed directly. In the case of CE, the lanthanides were extracted with bis(2-ethylhexyl)-ortho-phosphoric acid (HDEHP) (10) in toluene at pH = 2.0 and back-extracted into the aqueous phase using 6 mmol L^{-1} HNO_3. The HNO_3 solution was evaporated to dryness and the residues dissolved in 10 mL of water. The final solution was filtered through a 45-µm PTFE membrane syringe filter, and 35 nL of this solution was injected into the capillary.

RESULTS AND DISCUSSION

CE-ICP-MS for Lanthanide Determination

At first, it was observed that the make-up electrolyte solution, 0.005% v/v HNO_3, reduced the amount of HIBA and UV Cat-1 reagent to the ICP-MS, which minimized deposits on the interface of the ICP-MS spectrometer. Additionally, this solution displayed acceptable conductance and low background signals, improving the precision. As shown in Table III, the relative standard deviations (RSD) for 5 runs was lower than 10% for the different modes of signal measurement, but remarkably lower using peak area. Therefore, peak area was used to calculate the concentration of the separated lanthanides.

It was observed that both the position of the capillary in the nebulizer and the level of the make-up solution in the vessel (4) affect the peak shape and separation of the isotopes. Ions are separated by electric field application and the solution must not flow into the nebulizer CE capillary. Thus, it was very important to control these parameters in order to improve the separation. A CE-ICP-MS electropherogram of a 700-ng mL^{-1} standard of 13 lanthanide isotopes is shown in Figure 1. This electropherogram illustrates the low background signals and that the atomic ions signals of the lanthanides are separated.

Figure 2 illustrates a run where only Eu, Dy, and Er were monitored in a standard solution mixture containing 100 ng mL^{-1} of all lanthanides. The separation of polyatomic and isobaric species using CE prior to ICP-MS detection shows that that the interference is overcome.

Peak area information for each of the isotopes was used to calculate limits of detection (LODs) for the CE-ICP-MS method. The LOD was calculated as three times the standard deviation of the peak area observed for the blank, divided by the slope of the calibration curve. The LODs of most of the abundant isotopes ^{139}La, ^{141}Pr, ^{159}Tb, ^{165}Ho, ^{169}Tm, and ^{175}Lu were 7.6, 9.0, 5.4, 5.5, 10.1, and 11 µg L^{-1}, respectively. Lower abundance isotopes yield much smaller peak areas and are more difficult to detect and quantify by CE-ICP-MS. Day et al. (4) measured the abundance of lanthanide nuclides produced via spallation reactions on an irradiated tantalum target and illustrated that the method was applicable to the isotopes that were present in relevant concentrations. They reported LODs for the most abundant lanthanide isotopes in the range of 0.72 ng mL^{-1} to 3.9 ng mL^{-1} using CE coupled to a double focusing sector field ICP-MS. They also observed that the LODs were improved as much as one order of magnitude compared to a quadrupole ICP-MS.

TABLE III
Precision of CE-ICP-QMS for the Determination of Lanthanides Using the ELAN 6000 (PerkinElmer Sciex)

Isotope	Measurement Mode		
	Peak Area	Peak Width (1/2 Height)	Peak Height
	%RSD	%RSD	%RSD
^{139}La	3.1	5.8	8.4
^{141}Pr	2.6	6.7	2.9
^{159}Tb	3.0	7.3	3.2
^{165}Ho	1.5	5.4	8.3
^{169}Tm	3.5	5.2	7.6
^{175}Lu	2.9	3.6	3.9

Use of Micro Nebulizer With Desolvator for Lanthanide Determination in ICP-QMS

To accurately determine the low content of lanthanides, possible oxide formation must be considered because oxides of light lanthanides can interfere with lanthanide isotopes at m/z > 155. The argon gas flow rate to the nebulizer and the applied rf power have a large effect on the formation of oxide species, as well as ion intensity. For that reason, optimization was carried out in terms of nebulizer gas flow rate and rf power to maximize ion intensities of lanthanides and minimize oxide formation rate. The results of the optimization procedures are shown for La in Figure 3. It is important to mention that La was the element that exhibited the highest MO^+/M^+ value in comparison to the other lanthanides. It can be seen in Figure 3(a) that the MO^+/M^+ ratio at the optimized conditions is low (about 0.2%). The maximum sensitivity,

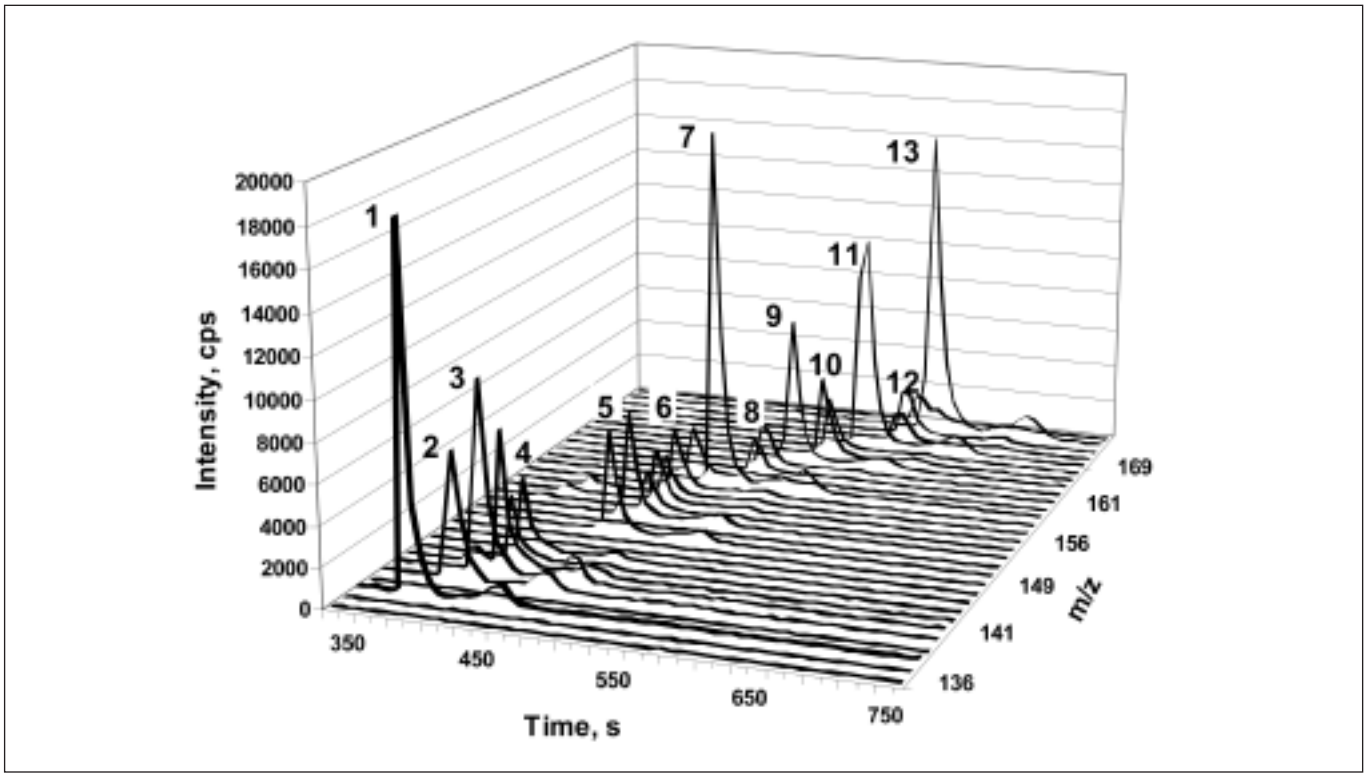

Fig. 1. CE-ICP-MS electropherogram of 700 ng mL^{-1} of lanthanides; 1: ^{139}La, 2: ^{140}Ce, 3: ^{141}Pr, 4: Nd isotopes, 5: Eu isotopes, 6: Gd isotopes, 7: ^{159}Tb, 8: Dy isotopes, 9: ^{165}Ho, 10: Er isotopes, 11: ^{169}Tm, 12: Yb isotopes and 13: ^{175}Lu.

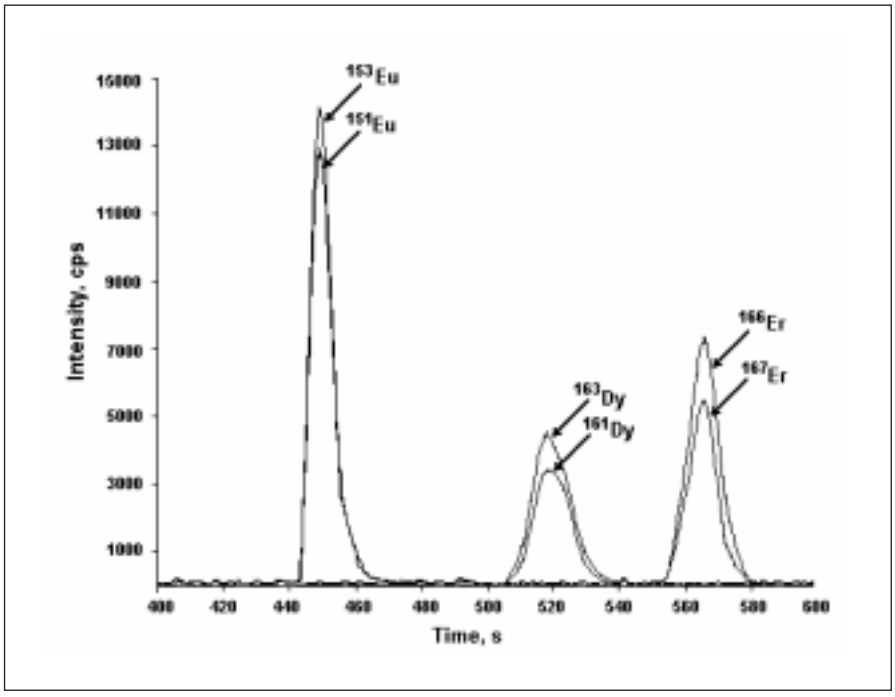

Fig. 2. CE-ICP-MS electropherogram of 100 ng mL^{-1} of lanthanides with m/z 156 through 164.

about 20 Mcps/mg L^{-1}, is achieved at a nebulizer gas flow rate of about 0.8 L min^{-1}, which remains almost the same up to1.5 L min^{-1} [Figure 3(b)]. The good performance is mainly due to the aerosol desolvation, which produces an intense and uniform dry aerosol, enhancing the sensitivity and precision as well. With respect to the effect of rf power on the oxide formation rate shown for La in Figure 3(c), it can be seen that the MO^+/M^+ ratio is lower than 0.004 at rf power in the range of 950 to 1500 W, whereas the sensitivity is practically constant at this interval [Figure 3(d)]. However, 950 W was chosen because it was observed that the sensitivities of other lanthanides (Sm, Eu, Er, Lu, Yb, and Dy) decreased at higher rf power.

The LODs obtained for the lanthanides by using the APEX system and ICP-MS are shown in Table IV.

Atomic Spectroscopy
Vol. 28(4), July/August 2007

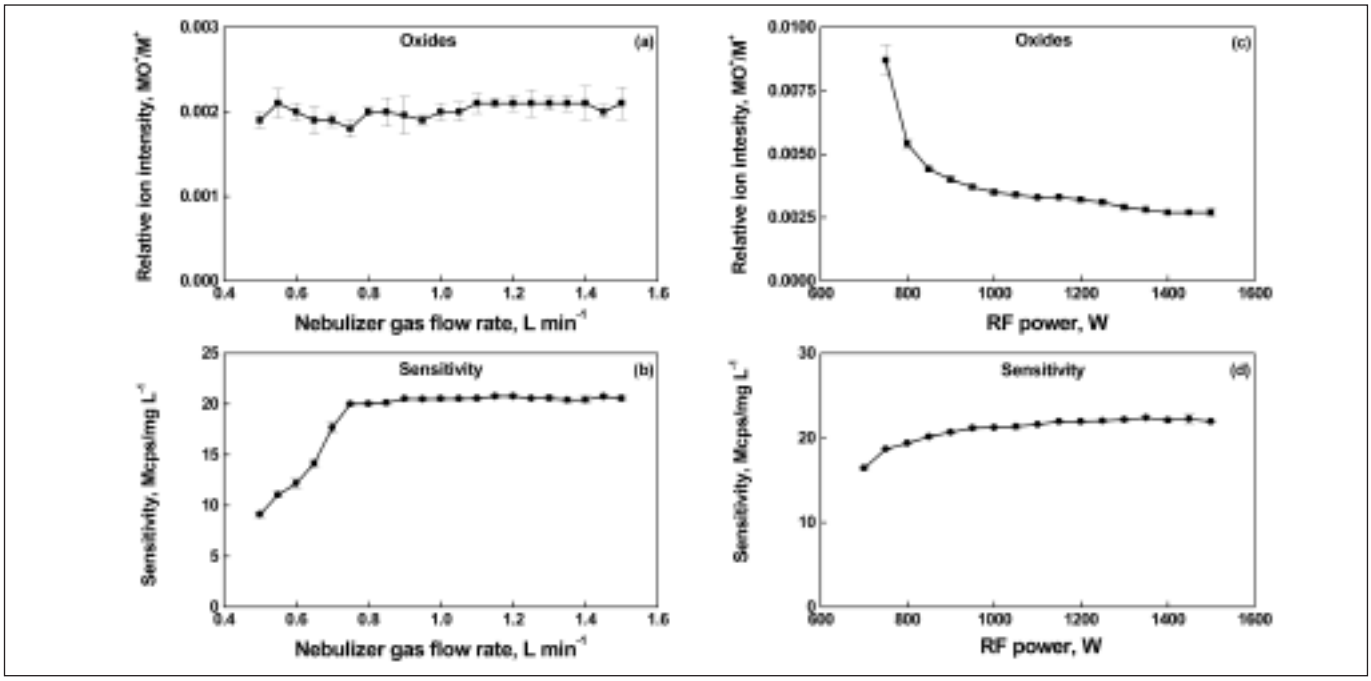

Fig. 3. Effect of nebulizer gas flow rate (rf power: 900 W) and rf power (nebulizer gas flow rate: 0.95 L min^{-1}) on the sensitivity and oxide formation rate (n = 3). Sample uptake rate: 330 µL min^{-1} and sample solution: 10 ng mL^{-1} La (M^+ and MO^+ represent the intensity of $^{139}La^+$ and $^{139}La^{16}O^+$, respectively).

TABLE IV
Limits of Detection (LODs) of Lanthanides Measured Using Micro Nebulizer-Desolvation System Coupled to ICP-QMS (ELAN 6100, PerkinElmer Sciex)

Isotope	LOD (ng L^{-1})	Isotope	LOD (ng L^{-1})
^{139}La	1.8	^{159}Tb	0.57
^{140}Ce	1.4	^{163}Dy	3.2
^{141}Pr	1.0	^{164}Ho	2.1
^{146}Nd	5.0	^{166}Er	3.5
^{152}Sm	1.6	^{169}Tm	1.8
^{153}Eu	2.2	^{172}Yb	3.7
^{156}Gd	6.1	^{175}Lu	0.85

They were obtained from 3 s, where s is the standard deviation of 10 consecutive measurements of the blank. The low LODs are mainly due to aerosol desolvation, which not only improves aerosol quality and minimizes oxide production, but also increases transport efficiency to the plasma. The good sensitivity and stability demonstrated that the system could be used for the determination of very low concentrations of lanthanides.

Lanthanide Concentrations in Mussel Tissue

The developed method was applied for lanthanide determination in certified mussel tissue (BCR 668), and the concentrations found are shown in Table V. The lanthanides are precisely detected in ICP-QMS using the micro nebulizer/desolvation system. All lanthanide concentrations measured are at the ng g^{-1} level and below. However, CE-ICP-MS could not be applied for these determinations since the concentrations of the lanthanides in the sample solution (at pg mL^{-1} level) were below the LODs of the method (at µg L^{-1} level). CE-ICP-MS can be applied for lanthanide determinations at higher concentration levels. It is useful when a small sample volume is available and serious interference problems occur with analyte ions, e.g., for analysis of radioactive materials (4,11).

CONCLUSION

It was demonstrated that CE-ICP-MS is a reliable technique for lanthanide separation prior to detection by ICP-MS, which reduces isobaric and polyatomic ion interferences. Nevertheless, the LODs are not sufficiently low for the determination of these elements naturally present in biological tissues. On the other hand, by using a micro nebulizer-desolvation system, which drastically reduces oxide formation and increases the sensitivity, the determination of low concentrations of lanthanides in biological samples is possible.

Received June 8, 2007.

TABLE V
Lanthanide Concentration Measured in Mussel Tissue (BCR 668) Using the Micro Nebulizer-Desolvation System for Introducing the Solution of the Digested Sample into the Plasma of the ICP-MS (n = 3, three replicates of the sample)

Element	Certified	Found	Element	Certified	Found
La	80 ± 6	85 ± 2	Gd	13.0 ± 0.6	12.0 ± 0.7
Lu	0.389 ± 0.024	0.363 ± 0.043	Tb	1.62 ± 0.11	1.44 ± 0.18
Ce	89 ± 7	85 ± 4	Dy	8.9 ± 0.6	7.9 ± 1.0
Pr	12.3 ± 1.0	12.1 ± 0.9	Ho[a]	1.8 ± 0.6	1.6 ± 0.3
Nd	54 ± 4	50 ± 1	Er	4.47 ± 0.45	3.78 ± 0.52
Sm	11.2 ± 0.8	12.3 ± 0.6	Tm	0.48 ± 0.08	0.38 ± 0.03
Eu	2.79 ± 0.15	3.02 ± 0.36	Yb[a]	2.8 ± 0.5	2.7 ± 0.02

[a]: Indicative values.

REFERENCES

1. J.S. Becker, Inorganic Mass Spectrometry. J. Wiley and Sons, Chichester, England (2007).
2. H.P. Longerich, B.J. Fryer, D.F. Strong, and C.J. Kantipuly, Spectrochim. Acta B 42, 75 (1987).
3. J.S. Becker and H.-J. Dietze, J. Anal. At. Spectrom. 12, 881 (1997).
4. J.A. Day, J.A. Caruso, J.S. Becker, and H.J. Dietze, J. Anal. At. Spectrom. 15, 1343 (2000).
5. Z.-H. Wang, X.-P. Yan, S.-P. Wang, Z.P. Zhang, and L-W. Liu, J. Am. Soc. Mass Spectrom. 17, 1258 (2004).
6. S. D'Ilio, N. Violante, S. Caime, D. Gregório, F. Petrucci, and O. Senofonte, Anal. Chim. Acta 432, 573 (2006).
7. S.F. Boulyga and K. Heumann, J. Environ. Radioact. 88, 1 (2006).
8. K.L. Ackley, J.A. Day, and J.A. Caruso, J. of Chromatogr. A 888, 293 (2000).
9. J.A. Day, K.L. Sutton, R.S. Soman, and J.A. Caruso, Analyst 125, 819 (2000).
10. V.K. Panday, K. Hoppstock, J.S. Becker, and H.J. Dietze, At. Spectrosc. 17, 98 (1996).
11. J.S. Becker, Inorganic Mass Spectrometry, Principles and Applications, Wiley & Sons, Chichester, U.K. (2007).

Influence of Organic and Inorganic Acids Commonly Used in Soil Extraction and Digestion Procedures in the Determination of Elements by Inductively Coupled Plasma Optical Emission Spectrometry

***Ana Paula Packer[a] and Maria Emília Mattiazzo**
Setor de Química, Departamento de Ciência Exatas
Escola Superior de Agricultura "Luiz de Queiroz", Universidade de São Paulo
Av. Pádua Dias, 11, CEP 13418-900, Piracicaba, SP, Brazil

ABSTRACT

Inductively coupled plasma optical emission spectrometers (ICP-OES) have been widely used to determine Cd, Co, Cr, Cu, Mg, Ni, Pb, and Zn in agronomic and environmental samples. However, sample preparation (as extraction and total digestion procedures) includes the use of some organic and inorganic acids not suitable for ICP analysis. It was found that the magnitude of the interferences is dependent on the ICP operating parameters. In order to achieve robust conditions, these parameters were adjusted. Robust conditions were verified by using the ratio of the ionic line intensity to the atomic line intensity of Mg, the most commonly used ratio for this purpose. Matrix effects of acetic, citric, hydrochloric, oxalic, nitric, perchloric, and tartaric acid in the determination of Cd, Co, Cr, Cu, Mg, Ni, Pb, and Zn for both robust and non-robust conditions were qualified using axial-view ICP-OES.

INTRODUCTION

Acids and easily ionized elements (EIE) play an important role in atomic spectrometric analysis because they are the most common matrices in agronomic and environmental samples analyzed by inductively coupled plasma optical emission spectrometry (ICP-OES), flame atomic absorption spectrometry (FAAS), and inductively coupled plasma mass spectrometry (ICP-MS) (1). Inorganic and organic acids are present in the sample solutions because they are widely used in sample preparation for plant, soil, and sediment total digestion (2). Also, a single reagent or a sequence of reagents is used in extraction procedures (3,4).

With the ICP-OES instrument, the ion formation in the central channel of the plasma can be detected using either the axial or radial view. The axial view configuration was developed to improve the observation efficiency of the central channel, while avoiding the surrounding intense Ar plasma (5). Compared to the radial view mode, the axial view presents an improvement factor in the range of 2 to 3 for several commercially available ICP-OES instruments (5) because of the enhancement of the analytical signal and reduction of the background signal. The decrease in the signal-to-background ratio (SBR) leads to an improvement of the limits of detection (LOD) (6–9). The axial view does present a higher matrix effect in the atomization zone, caused by easily ionized elements (EIE) (7,5), alkali and alkaline earth elements (14,10), and several acids (1,9,11). The matrix effects are due to different phenomena, such as a reduction in the aerosol transport efficiency because of the change in the aerosol density, an aerosol ionic redistribution in the spray chamber, and/or a change in the ICP atomization and excitation conditions (9).

The effect of inorganic acids and EIE in the ICP are known to cause signal suppression with increased acid concentration (12,13). Organic solvents can produce either enhancement or suppression of the signal depending on the type of solvent and the ICP equipment used (14).

Matrix effects from major elements (13,10) and acids (1) present in the sample solutions can be minimized by using adequate operational parameters, such as high power and low carrier gas, and the enlargement of the injector's internal diameter (15). By minimizing these matrix effects, the robust plasma is formed. That is, the temperature and the electron number density of the plasma are not modified during the analysis of the samples with matrices that can cause interferences (15). However, the analytical signal can still be affected by the transport and separation of the aerosol in the spray chamber (15,16). In matrix-effect related to aerosol problems, the elements seem to have the same behavior, which simplifies the use of internal standardization to compensate for accuracy degradation (17–19). To estimate whether the plasma is under robust conditions or not, the measurement of an ionic line to an atomic line intensity ratio is used. This is because the ionic lines are more sensitive to any change in the plasma condition than are atomic lines. Magnesium has been widely used for this purpose (16,20,21).

**Corresponding author.*
E-mail: apcpacker@terra.com.br
[a] Present address:
Instituto de Pesquisas Tecnológicas do Estado de São Paulo (IPT), Av. Prof. Almeida Prado, 532, CEP 05508-901, Cidade Universitária, São Paulo, SP, Brazil

The aim of this work was to study the influence of some organic and inorganic acids, used in the preparation of agronomic and environmental samples, on the signal behavior of the ionic and atomic lines in the ICP-OES determination of Cd, Co, Cr, Cu, Mg, Ni, Pb, and Zn. The interference of inorganic acids (hydrochloric, nitric, and perchloric) was evaluated because these acids are widely used to digest plant, soil, sediment, and several other samples. The effect created from the organic acids (tartaric, oxalic, citric, and acetic acid) on the analytical signal was investigated because of their importance in bioavailability studies of metals present in the soil.

EXPERIMENTAL

Instrumentation

The Optima™ 3000 XL inductively coupled plasma optical emission spectrometer with axial view (PerkinElmer Life and Analtyical Sciences, Shelton, CT, USA), equipped with a cross-flow nebulizer and a double pass Scott type spray chamber, was used to measure the elements. Sample solutions were propelled to the nebulizer by a peristaltic pump.

The instrumental operating parameters were changed to attain the robust conditions (Table I). Table II lists the lines used to measure Cd, Co, Cr, Cu, Mg, Ni, Pb, and Zn, the excitation energy of each line, as well as the energy sum, defined as the sum of ionization and excitation energy, for ionic lines.

For practical measurement of the Mg(II)/Mg(I) ratio, a factor of 1.7 was used to correct for a different wavelength response (20).

Reagents and Standard Solutions

Purified water (18.2 MΩ cm) produced using a Milli-Q™ system (Millipore, Bedford, MA, USA) was used to prepare the solutions. The acids used were tartaric ($C_4H_6O_6$), oxalic [$(COOH)_2 \cdot 2H_2O$], citric ($C_6H_8O_7$), ascorbic ($C_6H_8O_6$), nitric (HNO_3) 65% v/v ($d \simeq 1.40$), hydrochloric (HCl) 37% v/v ($d \simeq 1.19$), perchloric ($HClO_4$) 70% v/v ($d \simeq 1.68$), and acetic 99.7% v/v ($d \simeq 1.05$) (Merck, Darmstadt, Germany).

Solutions containing 5.0 mg L^{-1} of Cd, Co, Cr, Cu, Mg, Ni, Pb, and Zn in water and acids were prepared from a 1000-mg L^{-1} multi-element solution (ICP multi-element standard solution IV from Merck).

TABLE I
ICP-OES Instrumental and Operating Parameters Used to Determine the Matrix Effects of the Organic and Inorganic Acids

Plasma	
R.F. Power	1100 – 1500 W
Gas Flows:	
Plasma	15 L min^{-1}
Auxiliary	0.5 L min^{-1}
Nebulizer	0.45 – 1.0 L min^{-1}
Sample Flow Rate	1.0 mL min^{-1}
Injector Tube Diameter	2 mm
Measurements	50 s

TABLE II
Excitation Energy (E_{exc}) and Sum of Ionization and Excitation Energy (E_{sum}) for Atomic and Ionic Lines

Atomic Lines (nm)	E_{exc} (eV)	Ionic Lines (nm)	E_{exc} (eV)	E_{sum} (eV)
Cr I 357.869	3.46			
Cu I 324.754	3.82			
Co I 340.512	4.07			
Mg I 285.213	4.35			
Ni I 232.003	5.34			
Cd I 228.802	5.42			
Pb I 216.999	5.71			
Zn I 213.856	5.80	Zn II 202.548	6.12	11.91
		Mg II 280.270	4.42	12.07
		Cr II 267.716	6.15	12.92
		Co II 228.616	5.84	13.72
		Ni II 231.604	6.39	14.03
		Cd II 214.438	5.78	14.77
		Pb II 220.353	7.37	14.79
		Cu II 224.700	8.24	15.97

RESULTS AND DISCUSSION

The ionic [Mg(II) 280-nm] and atomic line [Mg(I) 285-nm] ratio intensities were used to determine the variation of the excitation and ionization conditions of the plasma (22,23). The plasma presents local thermodynamic equilibrium (LTE) conditions measured by Mg(II)/Mg(I). For the robust condition, the ratio values were higher than 8. To establish the robust condition of the axial view, ICP-OES was used, with Mg(II)/Mg(I) ratios measured by using rf powers of 1100, 1250, and 1550 W. The results were plotted as a function of the nebulization flow (Figure 1). For all nebulization flow rates, the plasma became more stable with an increase in rf power. At 1100 W, the robust condition was attained with a nebulization flow of 0.50 to 0.65 L/min. For 1250 and 1550 W, stable conditions were achieved using a nebulization flow between 0.45 and 0.70 L/min. For the following experiments, with robust condition (R), the rf power and nebulization gas flow used were 1500 W and 0.65 L/min, respectively, and for the non-robust conditions (NR), the parameters used were 1100 W and 1.0 L/min, respectively.

The influences of the organic and inorganic acid matrices were determined by measuring the pairs of ionic and atomic lines for the elements listed in Table II. The selection of Cd, Co, Cr, Cu, Mg, Ni, Pb, and Zn was based on their importance in agronomic and environmental studies.

The interference of inorganic acids in the determination of the chosen elements in robust (R) and non-robust (NR) conditions is shown in Figures 2 to 4. Independent of the plasma condition, all of the inorganic acids presented a signal reduction varying from 10% to 40%, compared with the atomic and ionic emission of the elements in water. The matrix effect in the

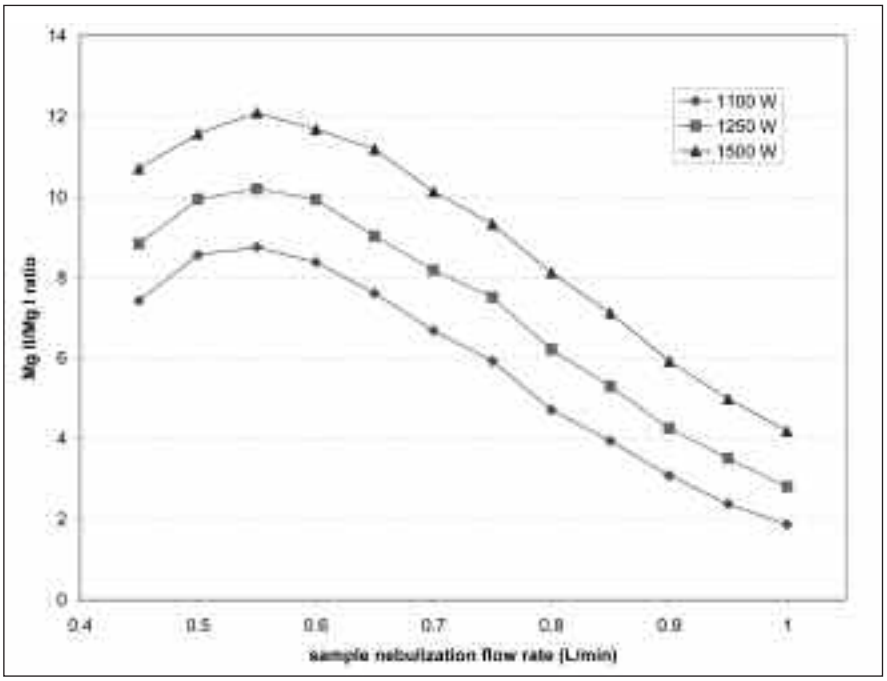

Fig. 1. Effect of the nebulization flow rate on the Mg II 280-nm/Mg I 285-nm line intensity ratio for rf power of 1100, 1250, and 1500 W.

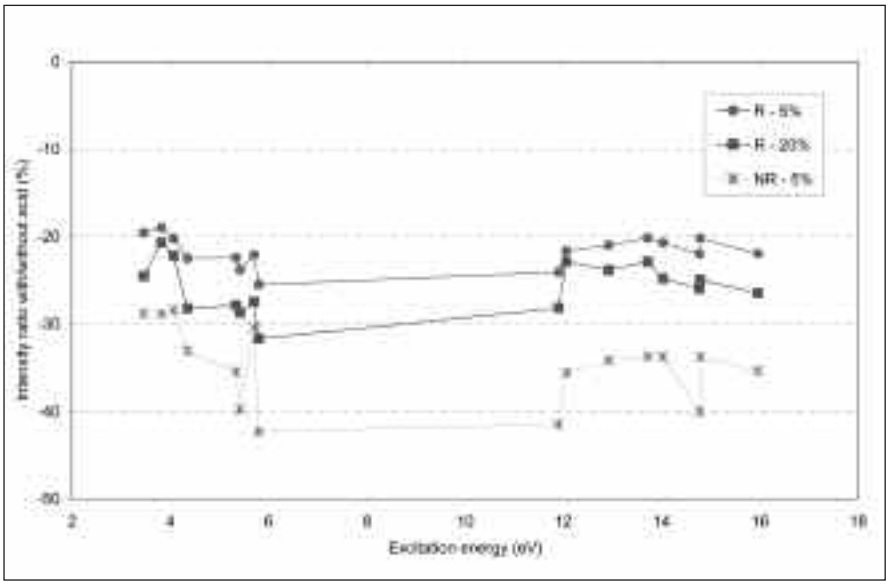

Fig. 2. Effect of 5% and 20% (v/v) nitric acid on the intensity of the atomic and ionic lines as a function of their energy of atomization or sum of the atomization plus the ionization energy (eV), in robust (R) and non-robust conditions (NR). Cr I (3.46 eV), Cu I (3.82 eV), Co I (4.07 eV), Mg I (4.35 eV), Ni I (5.34 eV), Cd I (5.42 eV), Pb I (5.71 eV), Zn I (5.80 eV), Zn II (11.91 eV), Mg II (12.07 eV), Cr II (12.92 eV), Co II (13.72 eV), Ni II (14.03 eV), Cd II (14.77 eV), Pb II (14.79 eV), Cu II (15.97).

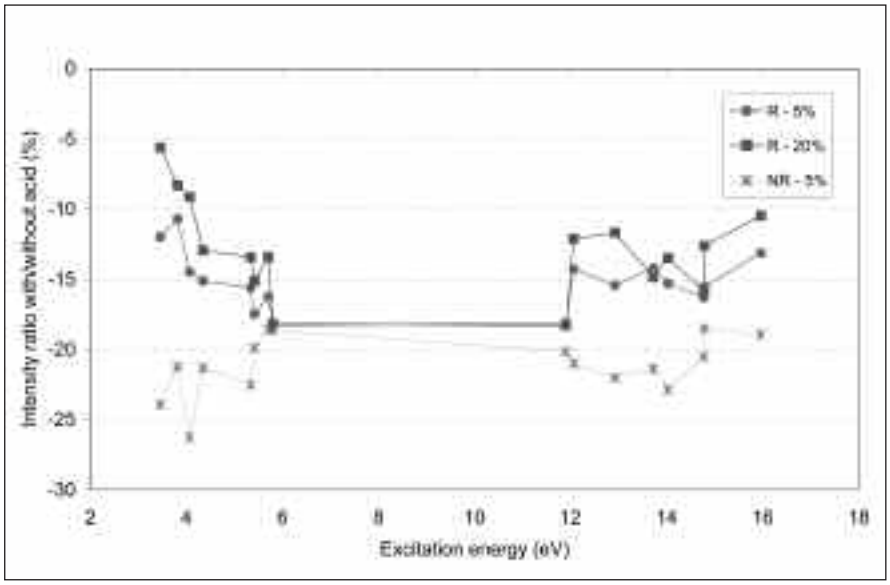

Fig. 3. Effect of 5% and 20% (v/v) hydrochloric acid on the intensity of the atomic and ionic lines as a function of their energy of atomization, or sum of the atomization plus the ionization energy (eV), in robust (R) and non-robust conditions (NR). Cr I (3.46 eV), Cu I (3.82 eV), Co I (4.07 eV), Mg I (4.35 eV), Ni I (5.34 eV), Cd I (5.42 eV), Pb I (5.71 eV), Zn I (5.80 eV), Zn II (11.91 eV), Mg II (12.07 eV), Cr II (12.92 eV), Co II (13.72 eV), Ni II (14.03 eV), Cd II (14.77 eV), Pb II (14.79 eV), Cu II (15.97).

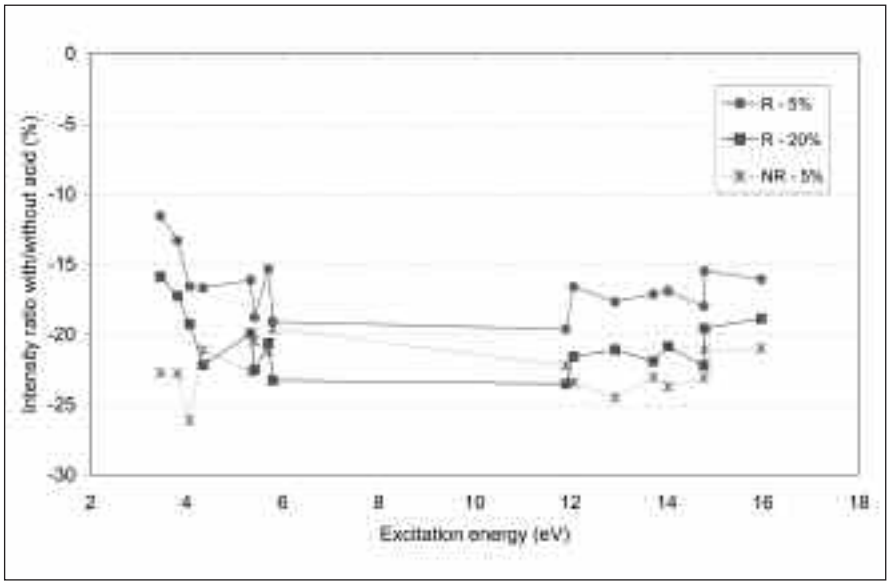

Fig. 4. Effect of 5% and 20% (v/v) perchloric acid on the intensity of the atomic and ionic lines as a function of their energy of atomization or sum of the atomization plus the ionization energy (eV), in robust (R) and non-robust conditions (NR). Cr I (3.46 eV), Cu I (3.82 eV), Co I (4.07 eV), Mg I (4.35 eV), Ni I (5.34 eV), Cd I (5.42 eV), Pb I (5.71 eV), Zn I (5.80 eV), Zn II (11.91 eV), Mg II (12.07 eV), Cr II (12.92 eV), Co II (13.72 eV), Ni II (14.03 eV), Cd II (14.77 eV), Pb II (14.79 eV), Cu II (15.97).

measured lines was higher for nitric acid. The signal suppression caused by nitric, hydrochloric, and perchloric acid was produced by the alterations in the thermal and excitation characteristics of the plasma (1,15,24). The decrease of the plasma temperature and the aspiration ratio with the enhancement of the acid concentration was related to an increase in the liquid viscosity. In non-robust conditions, the matrix effects caused by the acid in the plasma were enhanced.

Atomic Spectroscopy
Vol. 28(4), July/August 2007

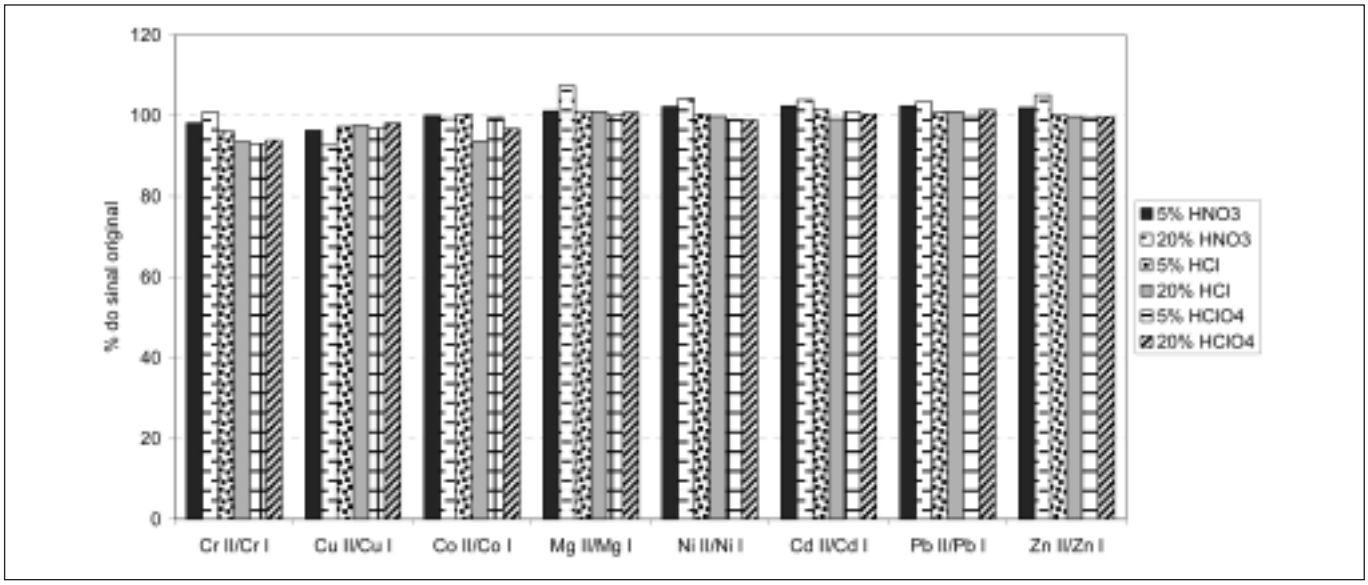

Fig. 5. Ionic and atomic emission signal ratio for Cr II/Cr I, Cu II/Cu I, Co II/Co I, Mg II/Mg I, Ni II/Ni I, Cd II/Cd I, Pb II/Pb I and Zn II/Zn I when analyzing 5% and 20% nitric (HNO_3), hydrochloric (HCl), and perchloric acid ($HClO_4$) matrices in robust conditions.

Ratios between the ionic and atomic lines for Cd, Co, Cr, Cu, Mg, Ni, Pb, and Zn were calculated to verify the origin of the interferences in the plasma, induced by inorganic acids, at 5% and 20% (v/v) for robust conditions (Figure 5). Variation from 95% to 105% in these ratios shows that the emission reductions produced by these matrices were similar for ionic and atomic lines, which indicates that the sample transport efficiency, through the introduction system and the plasma temperature, were decreased. For Co, Cr, and Cu, the ionic lines were more affected by the matrices than the atomic lines; these elements were also the ones with higher differences in the excitation energy for the atomic and ionic lines studied.

Oxalic, citric, and tartaric acid interferences in the ionic and atomic lines, for 1 and 2 mol/L, at robust (R) and non-robust (NR) conditions, are shown in Figures 6 to 8. For the organic acids, the sig-

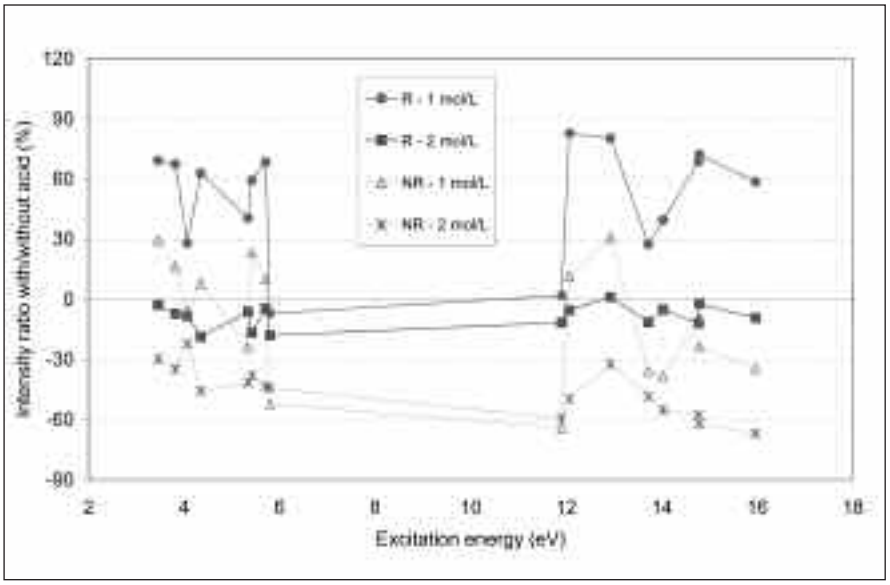

Fig. 6. Effect of 1 and 2 mol/L of oxalic acid on the intensity of the atomic and ionic lines as a function of their energy of atomization or sum of the atomization plus the ionization energy (eV), in robust (R) and non-robust conditions (NR). Cr I (3.46 eV), Cu I (3.82 eV), Co I (4.07 eV), Mg I (4.35 eV), Ni I (5.34 eV), Cd I (5.42 eV), Pb I (5.71 eV), Zn I (5.80 eV), Zn II (11.91 eV), Mg II (12.07 eV), Cr II (12.92 eV), Co II (13.72 eV), Ni II (14.03 eV), Cd II (14.77 eV), Pb II (14.79 eV), Cu II (15.97).

nal intensities for the chosen elements were decreased or increased depending on the choice and concentration of acid. The 2 mol/L acetic acid solution could not be measured (Figure 7), because at this concentration the plasma was extinguished due to the unstable condition created.

In robust conditions, 1 mol/L acetic and oxalic acid produced an increase on the emission signal of the Cd, Co, Cr, Cu, Mg, Ni, Pb, and Zn atomic and ionic lines (Figures 6 and 7). An exception was detected for the Zn atomic line (213.856 nm, excitation energy 5.8 eV) in oxalic acid, which showed a signal reduction of 7%. However, the emission signals were found to decrease with higher concentrations of oxalic acid.

The Cd(II) 214.438 nm (14.77 eV), Cr(II) 267.716 nm (12.92 eV), Mg(II) 280.270 nm (12.70 eV), Pb(II) 280.270 nm (14.79 eV), and Zn(II) 202.548 nm (11.91 eV) ionic line emissions were higher than the atomic lines for the oxalic and acetic acid analyses. Consequently, for these elements the ratios between the ionic and atomic lines (Figure 10) were higher than 100%, indicating that these acids were able to increase the thermal characteristics of the plasma and decrease the size of drop in the primary aerosol.

The introduction of citric and tartaric acid, at 1 and 2 mol/L, with robust plasma conditions decreased the emission signal for the ionic and atomic lines by 20% to 50% (Figures 8 and 9). For these matrices, the depreciation effect was higher for the Cr(I) 357.869 nm (3.46 eV), Mg(I) 285.213 nm (4.35 eV), Ni(I) 232.003 nm (5.34 eV), Cd(I) 228.802 nm (5.42 eV), Pb(I) 216.999 nm (5.71 eV), and Zn(I) 213.856 nm (5.80 eV) atomic lines, and also for the Co(II) 228.616 nm (13.72 eV) and Cu(II) 224.700 nm (15.97 eV) ionic lines. The decrease in the emission signal for the above

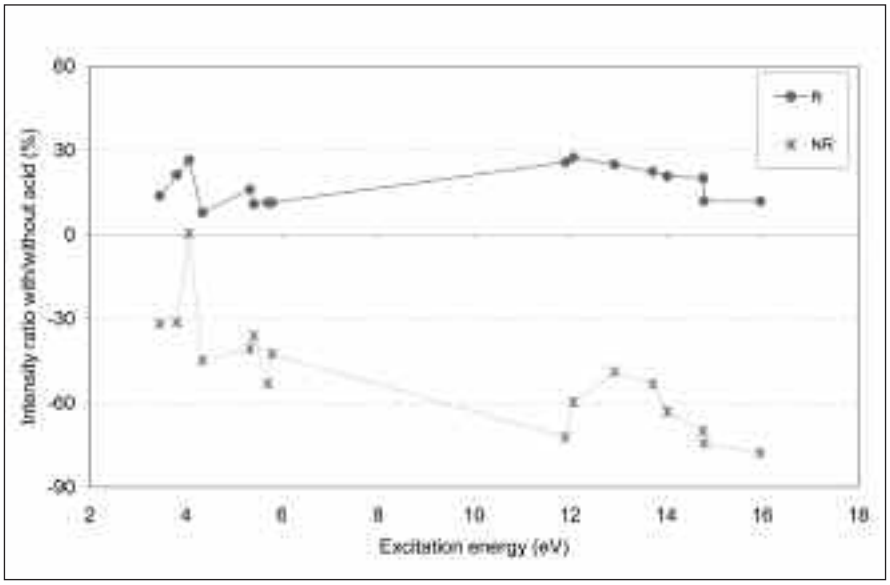

Fig. 7. Effect of 1 mol/L of acetic acid on the intensity of the atomic and ionic lines as a function of their energy of atomization or sum of the atomization plus the ionization energy (eV), in robust (R) and non-robust conditions (NR). Cr I (3.46 eV), Cu I (3.82 eV), Co I (4.07 eV), Mg I (4.35 eV), Ni I (5.34 eV), Cd I (5.42 eV), Pb I (5.71 eV), Zn I (5.80 eV), Zn II (11.91 eV), Mg II (12.07 eV), Cr II (12.92 eV), Co II (13.72 eV), Ni II (14.03 eV), Cd II (14.77 eV), Pb II (14.79 eV), Cu II (15.97).

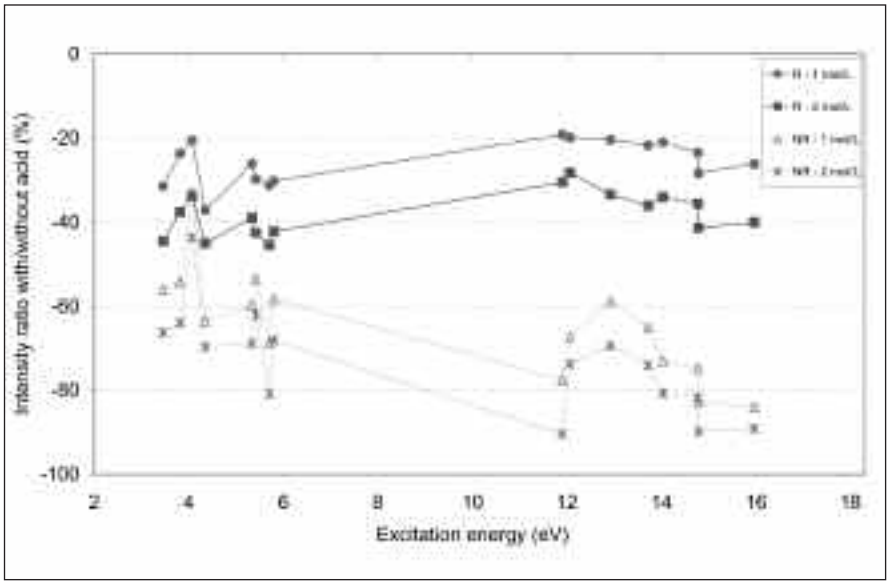

Fig. 8. Effect of 1 and 2 mol/L of citric acid on the intensity of the atomic and ionic lines as a function of their energy of atomization or sum of the atomization plus the ionization energy (eV), in robust (R) and non-robust conditions (NR). Cr I (3.46 eV), Cu I (3.82 eV), Co I (4.07 eV), Mg I (4.35 eV), Ni I (5.34 eV), Cd I (5.42 eV), Pb I (5.71 eV), Zn I (5.80 eV), Zn II (11.91 eV), Mg II (12.07 eV), Cr II (12.92 eV), Co II (13.72 eV), Ni II (14.03 eV), Cd II (14.77 eV), Pb II (14.79 eV), Cu II (15.97).

lines and the atomic-to-ionic lines ratios (Figure 10) indicates that the nebulization system efficiency was diminished with the introduction of these matrices in comparison to water nebulization.

CONCLUSION

Matrix interferences in ICP-OES measurement are more significant in non-optimized operating conditions.

Robust conditions of the ICP-OES are not sufficient to suppress the matrix effects of nitric, hydrochloric, perchloric, citric, tartaric, oxalic, and acetic acid in the plasma. Nitric, hydrochloric, perchloric, citric, and tartaric acid decreases the analytical signal produced by the inefficient aerosol production, and diminishes the temperature of the plasma. However, use of acetic and oxalic acid increases the emission signals of

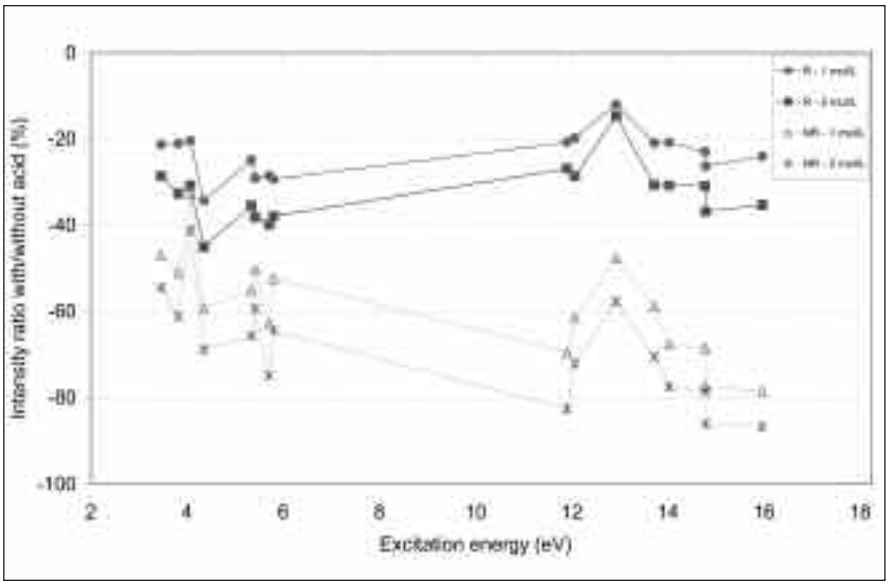

Fig. 9. Effect of 1 and 2 mol/L of tartaric acid on the intensity of the atomic and ionic lines as a function of their energy of atomization or sum of the atomization plus the ionization energy (eV), in robust (R) and non-robust conditions (NR). Cr I (3.46 eV), Cu I (3.82 eV), Co I (4.07 eV), Mg I (4.35 eV), Ni I (5.34 eV), Cd I (5.42 eV), Pb I (5.71 eV), Zn I (5.80 eV), Zn II (11.91 eV), Mg II (12.07 eV), Cr II (12.92 eV), Co II (13.72 eV), Ni II (14.03 eV), Cd II (14.77 eV), Pb II (14.79 eV), Cu II (15.97).

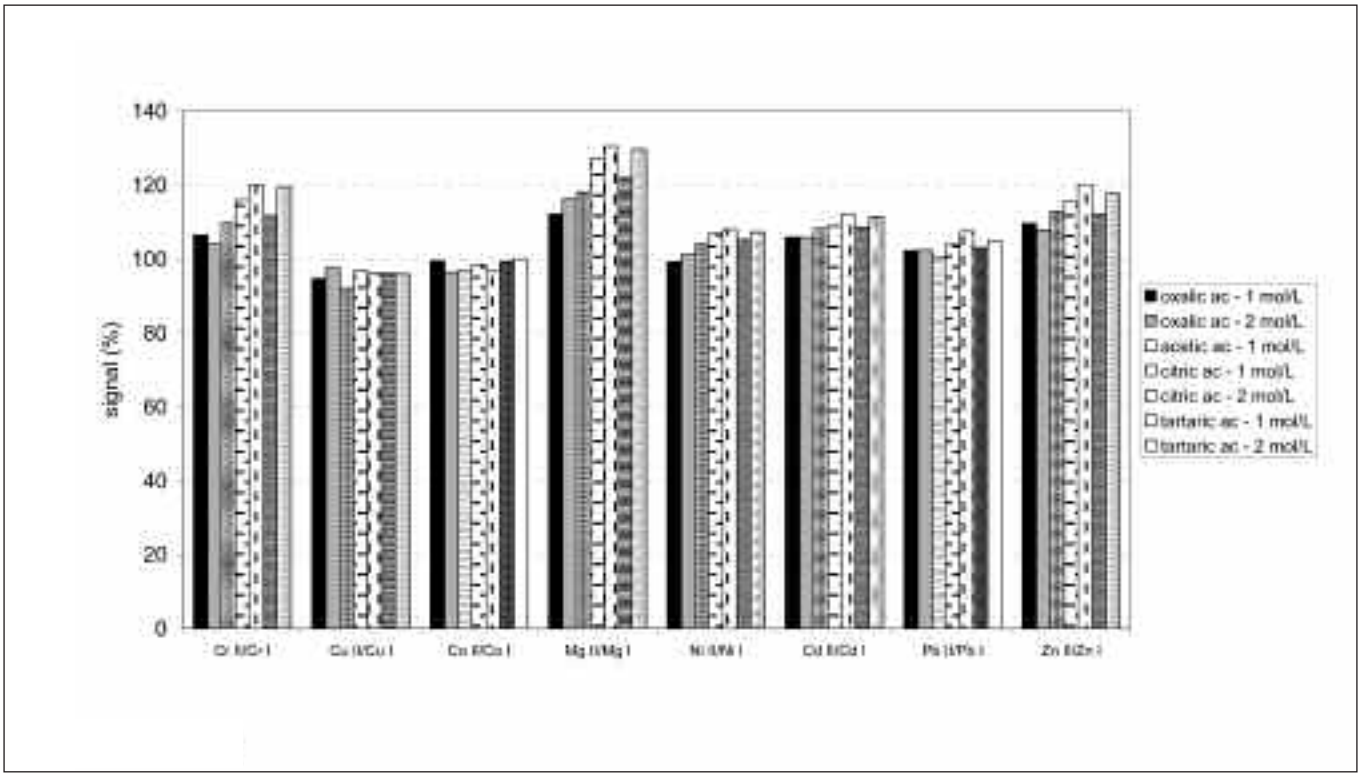

Fig. 10. Ionic and atomic emission signal ratio for Cr II/Cr I, Cu II/Cu I, Co II/Co I, Mg II/Mg I, Ni II/Ni I, Cd II/Cd I, Pb II/Pb I and Zn II/Zn I when analyzing 1 and 2 mol/L of tartaric, citric, oxalic and acetic acid in robust conditions.

the ionic and atomic lines, and also increases the ratio between the lines. These matrices enhance the thermal characteristics of the plasma and diminish the size of drops in the primary aerosol.

ACKNOWLEDGMENTS

The authors wish to thank FAPESP (Fundação de Amparo a Pesquisa do Estado de São Paulo) for the financial support.

Received March 12, 2007.

REFERENCES

1. J.L. Todoli and J.M. Mermet, Spectrochim. Acta 13, 895 (1999).
2. I. Lavilla, A.V. Filgueiras, and C. Bendicho, J. Agric. Food Chem. 47, 5072 (1999).
3. A.M.M. Pires and M.E. Mattiazzo, Sci. Agric. 60, 161 (2003).
4. P.C.F.C. Gardolinski, A.P. Packer, C.R. de Almeida, and M.F. Gine, J. Braz. Chem. Soc. 13, 375 (2002).
5. C. Dubuisson, E. Poussel, and J.M. Mermet, J. Anal. At. Spectrom. 12, 281 (1997).
6. Y. Nakamura, K. Takahashi, O. Kujirai, H. Okochi, and C.W. McLeod, J. Anal. At. Spectrom. 9, 751 (1994).
7. I.B. Brenner, A. Zander, M. Cole, and A. Wiseman, J. Anal. At. Spectrom. 12, 897 (1997).
8. W. Schron and A. Liebmann, Fresenius J. Anal. Chem. 361, 207 (1998).
9. C. Dubuisson, E. Poussel, J.M. Mermet, and J.L. Todoli, J. Anal. At. Spectrom. 13, 63 (1998).
10. I.B. Brenner, S. Vats, and A.T. Zander, J. Anal. At. Spectrom. 14, 1231 (1999).
11. J.L. Todoli, J.M. Mermet, A. Canals, and V. Hernandis, J. Anal. At. Spectrom. 13, 55 (1998).
12. I.I. Stewart and J.W. Olesik, J. Anal. At. Spectrom. 13, 1313 (1998).
13. C. Dubuisson, E. Poussel, and J.M. Mermet, J. Anal. At. Spectrom. 13, 1265 (1998).
14. I.B. Brenner, M. Zischka, B. Maichin, and G. Knapp, J. Anal. At. Spectrom. 13, 1257 (1998).
15. M. Stepan, P. Musil, E. Poussel, and J.M. Mermet, Spectrochim. Acta 56B, 443 (2001).
16. J.M. Mermet, J. Anal. At. Spectrom. 13, 419 (1998).
17. X. Romero, E. Poussel, and J.M. Mermet, Spectrochim. Acta 52B, 487 (1997).
18. J.C. Ivaldi and J.F. Tyson, Spectrochim. Acta 51B, 1443 (1996).
19. P. Masson, Spectrochim. Acta 54B, 603 (1999).
20. J. Dennaud, A. Howes, E. Poussel, and J.M. Mermet, Spectrochim. Acta 56B, 101 (2001).
21. J.C.J. Silva, N. Baccan, and J.A. Nóbrega, J. Braz. Chem. Soc. 14, 310 (2003).
22. J.M. Mermet, Spectrochim. Acta 44B, 1109 (1989).
23. J.M. Mermet, Anal. Chim. Acta 250, 85 (1991).
24. S. Greenfield, H.M. McGeachin, and P.B. Smith, Anal. Chim. Acta 84, 67 (1976).

Aqueous and Acidified Slurry Sampling Approaches in the As, Sb, and Sn Determination of Urban Dust Samples by HG-ETAAS

***Jorge Moreda-Piñeiro[a], Carmen Moscoso-Pérez[a], María Piñeiro-Iglesias[b], Purificación López-Mahía[a,b], Soledad Muniategui-Lorenzo[a], Esther Fernández-Fernández[a], and Darío Prada-Rodríguez[a,b]**

[a] Department of Analytical Chemistry, Faculty of Sciences, University of A Coruña, Campus da Zapateira s/n. E-15071, A Coruña, Spain

[b] University Institute of Environment, University of A Coruña, Pazo de Lóngora, E-15179, Oleiros, Spain

ABSTRACT

Conventional solid sample pre-treatments for metals determination by spectroscopy methods involve several disadvantages. To overcome these limitations, an alternative sample pre-treatment such as slurry sampling is being proposed. A critical study of the use of aqueous and acidified slurry sampling techniques was carried out for the direct determination of As, Sb, and Sn in local urban dust samples and a standard reference material, NIST SRM 1649a Urban Dust, by hydride generation coupled with electrothermal atomic absorption spectrometry. The values determined were compared with the certified values of the NIST sample. The values obtained from local urban dust samples were compared with the values achieved by a conventional method based on an acid digestion followed by ICP-MS determination.

The influence of mean particle size, chemical composition, and analyte oxidation state were also studied. The recoveries using aqueous slurry sampling for NIST SRM 1649a Urban Dust were 83% and 110% for As and Sn, respectively; however, low recovery (22%) was achieved for Sb. On the other hand, the recoveries using acidified slurry sampling of NIST SRM 1649a were close to 100% for the hydride-forming elements. The recoveries obtained using aqueous and acidified slurry sampling of the local urban dust samples ranged from 29–41 % for As, 32–66 % for Sb, and 76–81% for Sn from aqueous slurries, and 90–100 % for all target metals from acidified slurries.

INTRODUCTION

During the last few decades, human activities have introduced significant amounts of heavy metals into the environment. Anthropogenic emission of metals such as As, Sb, and Sn are higher than by natural occurrence. These metals are released into the atmosphere from the smelting of metals, combustion of coal and fossil fuels, use of pesticides, and as a consequence of several industrial processes (1). They are transported into the atmosphere over long distances and then accumulate in soil, plants, mosses, etc. Coal ashes are also a significant source of metals which leach into waters or the soil. Different international bodies and governments have regulated some pollutant levels to protect human health. For instance, for air quality, the European Commission Directive 2004/107/EC (2) fixed an annual target value of 6 ng m^{-3} for As.

The most widely used methods for determining the As, Sb, and Sn content of particulate matter and urban dust are based on the hydride generation technique followed by analysis with atomic absorption (3–4), atomic emission (5–7), or atomic fluorescence spectrometry (8–10). Simplicity, high sensitivity, and relative freedom from interferences are the main advantages of this approach. Although hydride techniques are convenient for measuring gas phase hydride-forming elements, the samples must first be digested to reduce the elements and then aerated to liberate the hydrides into the gas phase. Solid samples are subsequently digested in an acid mixture by mechanical agitation, ultrasonic or microwave treatment, followed by hydride generation coupled to spectrometric analysis. The major disadvantages of these conventional pre-treatments are that they involve several sample handling steps which require ultra-clean sampling techniques and clean room facilities to avoid contamination. Moreover, it is a very tedious and time-consuming process. In addition, these procedures use toxic acids at high concentrations during the sample pre-treatment which are not environmentally friendly.

To overcome these limitations, alternative sample pre-treatments have been proposed, including direct hydride generation from solid particles of several slurried samples such as marine sediment, soil, coal, coal fly ash, pigments, and powdered food samples (11). The avoidance of sample acid extraction procedures is the main advantage of these procedures. By using the slurry approach, sample pretreatment time is highly minimized. In addition, the possibility for analyte loss and sample contamination is reduced.

The aim of this work was to study the possibility of using direct hydride generation for aqueous and acidified slurries of a standard refer-

**Corresponding author.*
E-mail: jmoreda@udc.es
Tel: +34 – 981-167000 Ext. 2062
Fax: +34 – 981-167065

ence material NIST SRM 1649a Urban Dust and urban dust samples collected in the areas of A Coruña (NW Spain). The values obtained by the slurry approach were compared with the certified or indicative values. The differences in the results are due to the chemical composition and the mean particle size of samples. Element determination and X-ray diffractometry (XRD) were used for chemical composition analysis of both samples (urban dust reference material and local urban dust samples). The target analytes As, Sb, and Sn were measured by hydride generation coupled to electrothermal atomic absorption spectrometry (HG-ETAAS) and using Ir-treated graphite tubes.

EXPERIMENTAL

Instrumentation

A Model AAnalyst™ 800 atomic absorption spectrometer (PerkinElmer Life and Analytical Sciences, Shelton, CT, USA), equipped with electrodeless discharge lamps (EDL System 2), was used to determine arsenic, antimony, and tin. The operating conditions are listed in Table I. A Model MHS-10 hydride generation system (PerkinElmer) was used for hydride generation. Pyrolytically coated graphite tubes (THGA™ graphite tubes, PerkinElmer) with Ir-treated pyrolytic platforms were used. An integrated absorbance signal was used throughout.

Reagents and Standard Solutions

All solutions were prepared from analytical reagent grade chemicals using ultra-pure water with a resistivity of 18 MΩ cm^{-1}, obtained from a Milli-Q™ water purification system (Millipore, Bedford, MA, USA). Arsenic, antimony, and tin stock standard solutions, 1000 mg/L (Panreac, Barcelona, Spain) were used. Potassium iodide (Merck, Darmstadt, Germany) was used for Sb pre-reduction. Sodium tetrahydroborate (Aldrich, Milwaukee, WI, USA), dissolved in 0.5% (w/v) of sodium hydroxide (Panreac), was used as the reducing solution. This solution was prepared daily and filtered before use. Diluted hydrochloric acid solution (6.0 M) was prepared from hydrochloric acid solution, 37% (Panreac). Nitric acid 69–70% (Baker, Phillipsburg, PA, USA), hydrofluoric acid 48–51% (Baker), and perchloric acid 69–72% (Baker) were used for acid digestion. SRM 1649a Urban Dust reference material was obtained from the National Institute of Standards and Technology (Gaithersburg, MD, USA). Argon C-45 purity (99.995%) (Carburos Metálicos, Barcelona, Spain) was used as the purge gas.

Local Urban Dust Sample Collection and Preparation

Dust samples were collected in an urban (latitude 43°22'02''N, longitude 8°25'10''W) and suburban (latitude 43°12'00''N, longitude 8°10'12''W) area of A Coruña city (NW Spain) using a filter bag and a vacuum cleaner. The material was removed from the filter bag and then passed through a 200-mesh sieve to remove bag fibers and other extraneous materials. The sieved material was then thoroughly mixed and bottled.

TABLE I
Optimum Spectrometer, Hydride Generation, Trapping and Atomization Conditions for Direct As, Sb, and Sn Determination From Aqueous and Acidified Slurries by HG-ETAAS

Spectrometer Operating Conditions			
	Wavelength (nm)	Slit Width (nm)	Lamp Current (mA)
As	193.7	0.7	380
Sb	217.6	0.2	410
Sn	286.3	0.7	325

Hydride Generation Conditions				
	HCl (mol/L)	$NaBH_4$ (% w/v)	Reaction Volume (mL)	Ar Flow Rate (mL/min)
As	0.5	1.0	5.0	50
Sb	1.0	1.0	5.0	50
Sn	0.5	1.0	5.0	50

Trapping and Atomization Conditions					
	Step	Temp. (°C)	Ramp (s)	Hold (s)	Ar Flow Rate (mL/min)
As	Collection	800	1	30	250
	Atomization	2000	0	3	0 (read)
	Cleaning	2300	1	3	250
Sb	Collection	500	1	30	250
	Atomization	1900	0	5	0 (read)
	Cleaning	2300	1	3	250
Sn	Collection	1000	1	30	250
	Atomization	2000	0	3	125 (read)
	Cleaning	2300	1	3	250

Aqueous and Acidified Slurry Preparation

A 0.2500-g portion of each sample and appropriate volumes of glycerol were diluted to 25 mL with Milli-Q water for preparation of the aqueous slurry. The glycerol concentration, after diluting to 25 mL, was 0.2% (v/v). This concentration allows an adequate stability of the slurry.

A 0.2500-g portion of each sample was mixed with adequate HNO_3 volumes to reach a concentration of 4.0 M after dilution to 25 mL for preparation of the acidified slurry.

The aqueous and acidified slurries were kept in polyethylene vials at 4 °C. A 1:10 dilution of these slurries was required for As determination due to the high sensitivity of the proposed method and the relatively high As concentration in the NIST SRM 1649a samples.

Procedure for Slurry Measurements by HG-ETAAS

Hydride generation was produced in a 100-mL reaction vessel. Different aqueous or acidified slurry volumes were introduced into the reaction vessels with adequate volumes of hydrochloric acid (6.0 M) and then diluted to 5.0 mL with Milli-Q water (Table I). The tip of the quartz capillary tube from the outlet of the batch hydride generation system was inserted into the center of the graphite tube. PerkinElmer software (WinLab^{32TM} for AA) was used for automated hydride trapping into the Ir-treated graphite tubes. The hydride generated by the addition of sodium tetrahydroborate was then carried by the purge gas flow to the furnace where it was sequestered onto the heated Ir-treated graphite tube. Then, the quartz capillary moves out of the graphite tube. The trapped analyte was atomized during 3.0 seconds for As and Sn determination and 5.0 seconds for Sb determination using maximum heating power. Internal gas stop for all hydride elements was studied except for Sn when the NIST samples were analyzed. An Ar flow rate of 125 mL min^{-1} was necessary during atomization for the Sn determination in the NIST samples due to the high tin content. The optimum vapor generation, trapping, and atomization conditions obtained for each species are listed in Table I.

Procedure for HG-ETAAS Analysis of Local Urban Dust Acid Digests

A 0.2500-g portion of the local urban dust samples was digested after validating the method (by analyzing the NIST 1649a Urban Dust reference material) as described by Querol et al. (12). Urban dust acid extracts were analyzed by HG-ETAAS using the conditions listed in Table I.

Optimization of Hydride Generation and ETAAS Detection Conditions

Different experiments were carried out to establish the optimum conditions for hydride generation and hydride adsorption onto the Ir-treated graphite tubes from aqueous and acidified slurries of SRM 1649a Urban Dust standard reference material. The influence of various hydrochloric acid and sodium tetrahydroborate concentrations on the efficiency of hydride generation was studied in the range of 0.25–1.5 M and 0.5–2.0% (m/v), respectively. The variables of trapping temperature, atomization temperature, trapping time, and Ar flow rate were also optimized. The studied ranges were 25–1000 °C, 1800–2500 °C, 10–60 s, and 20–60 mL min^{-1} for trapping temperature, atomization temperature, trapping time, and Ar flow rate, respectively. The optimum values obtained for the studied factors are listed in Table I.

Features of the Methods

Table II shows the calibration and addition equations obtained for several metals studied. Slurry portions were spiked with 0.1, 0.2, and 0.4 µg L^{-1} of As(III), or with 0.25, 0.5, and 1.0 µg L^{-1} of Sb(III), or with 2.0, 4.0, and 6.0 µg L^{-1} of Sn for As, Sb, and Sn determination, respectively. As we can see, for each analyte the slopes of the calibration and standard addition graphs are not statistically similar (*t*-test for a confidence level of 95.0%). Therefore, matrix effect is important and the standard addition method must be used. The detection and quantification limits, defined as 3Sd/m and 10Sd/m, respectively; where Sd is the standard deviation of 11 measurements of a blank and m is the slope of the addition graphs, are also listed in Table II. The within-batch precision (relative standard deviation of 11

TABLE II
Features of the Determination Methods

	Calibration	Addition NIST SRM 1649a	Addition Local Urban Dust	LOD (µg g^{-1})	LOQ (µg g^{-1})
As	QA=0.069+0.528[As]	QA=0.178+0.460[As]	QA=0.192+0.752[As]	3.5	12.0
Sb	QA=0.034+0.243[Sb]	QA=0.115+0.214[Sb]	QA=0.142+0.336[Sb]	0.3	0.8
Sn	QA=0.120+0.030[Sn]	QA=0.241+0.022[Sn]	QA=0.194+4 10-3[Sn]	2.0	6.5

replicate measurements at different concentration levels) obtained for the different hydride generation procedures were good; the RSD (%) was lower than 7.5% for all concentrations studied.

RESULTS AND DISCUSSION

Table III lists the As, Sb, and Sn concentrations in NIST SRM 1649a Urban Dust using aqueous and acidified slurries, expressed as

$$\bar{x} \pm \frac{t_{(0.05,\,10)}\,\mathrm{Sd}}{\sqrt{n}}$$

where $\bar{x}$ and Sd are the mean and the standard deviation for n = 11 measurements; $t_{(0.05,10)}$ is the Student's *t*-test for n – 1 = 10 degrees of freedom and at a confidence level of 95% [$t_{(0.05,10)} = 2.23$]. Table IV also lists the As, Sb, and Sn concentrations in the dust samples collected from urban and suburban areas of A Coriña, NW Spain, expressed as discussed above.

Aqueous Slurries of NIST SRM 1649a and Local Urban Dust

Good recoveries (83–110%), relative to the certified values of NIST SRM 1649a Urban Dust, for As and Sn were obtained when aqueous slurries were used (Table III). By using the conditions described in the Procedure section, As and Sn could easily pass from the particles to the liquid media and react with sodium tetrahydroborate. Thus, direct As and Sn hydride generation from the aqueous slurries of the NIST sample (without acid pretreatment) is a viable approach.

Low recovery (22%) was achieved for Sb from NIST SRM 1649a using aqueous slurry sampling. The pentavalent oxidation state of Sb is the predominant antimony species in the atmospheric particulate (8). Thus, the low recovery percentages could be due to the poor hydride generation efficiency obtained when the antimony hydride is generated from the pentavalent oxidation state (13). On the other hand, the high affinity between Sb and the matrix sample could also explain the low Sb hydride generation efficiency.

A study of the influence of the oxidation state on the antimony hydride generation was carried out. The optimized procedure described in the Procedure section was modified as follows: Several potassium iodide concentrations in the range of 0.05 to 0.1 M were mixed into the reaction vessel with the slurry sample and hydrochloric acid before adding the sodium tetrahydroborate. Thus, Sb(V) is reduced to Sb(III) by the potassium iodide in an acid medium and the hydride is generated from the trivalent oxidation state by the reaction with sodium tetrahydroborate. The results obtained using this modified procedure offer similar recoveries and we can conclude that Sb is strongly bonded to the matrix sample. Thus, the antimony content in solid particles cannot pass to the liquid media using the proposed conditions.

As can be seen in Table IV, low recoveries were obtained for As (29–41%), Sb (32–66%), and Sn (76–81%) from the aqueous slurry of the local urban dust samples. The reference values used to achieved those recoveries are the As, Sb and Sn concentrations obtained by ICP-MS after acid digestion (Table IV). The low recovery percentages found in these samples could be a consequence of a different chemical composition and/or of a different mean particle size in comparison to the NIST sample.

TABLE III
Analysis of NIST SRM 1649a Urban Dust Using Aqueous and Acidified Slurries (N = 11)

	Certified Value (μg g^{-1})	Found Value (μg g^{-1})	
		Aqueous Slurry	Acidified Slurry
As	67 ± 2	53 ± 2	70 ± 3
Sb	29.9 ± 0.7	6.6 ± 0.6	28.3 ± 1
Sn	56 ± 13	62 ± 5	63 ± 3

TABLE IV
Analysis of Local Urban Dust Samples Using Aqueous and Acidified Slurries (Slurries prepared from non-pulverized samples, N =11.)

	Acid Digestion-ICP-MS[a] (μg g^{-1})	Local Urban Dust (μg g^{-1})	
		Aqueous Slurry	Acidified Slurry
As	12.5 ± 0.6	5.1 ± 0.2	11.7 ± 0.2
Sb	10.7 ± 0.4	7.1 ± 0.3	9.9 ± 0.2
Sn	16.6 ± 0.3	13.4 ± 0.5	17.2 ± 0.5
	Acid Digestion-ICP-MS[a] (μg g^{-1})	Local Sub-urban Dust (μg g^{-1})	
		Aqueous Slurry	Acidified Slurry
As	9.7 ± 0.2	2.8 ± 0.1[b]	9.0 ± 0.3
Sb	10.4 ± 0.3	3.3 ± 0.2[c]	9.5 ± 0.4
Sn	20.1 ± 0.4	15.2 ± 0.6[d]	20.5 ± 0.5

[a] According to procedure described in Reference 12.
[b] 6.3 ± 0.2 μg g^{-1} for pulverized sample.
[c] 5.2 ± 0.2 μg g^{-1} for pulverized sample.
[d] 17.1 ± 0.4 μg g^{-1} for pulverized sample.

Atomic Spectroscopy
Vol. 28(4), July/August 2007

Complementary analysis was carried out to establish the chemical composition of NIST SRM 1649a and the local urban dust samples. Chemical composition was performed by element analysis (Carlo-Erba CHNS-O EA 1108, Milan, Italy) and X-ray diffraction (Siemens D5000 diffractometer, Karlsruhe, Germany). The differences in chemical composition of these matrices could explain the low hydride generation efficiency obtained when aqueous slurries of the local urban dust samples were analyzed.

From the elemental analysis data (Table V) we can conclude that N, C, H, and S percentages are lower in the local urban and suburban dust samples than in the NIST reference material. The low carbon percentage in the local urban dust samples could explain the poor hydride generation efficiency as compounds, minerals, and particles containing carbon are easily digested using the hydrochloric acid concentration required to generate the hydride. Thus, metals pass to the liquid media and react with sodium tetrahydroborate. In addition, the high specific surface area of the carbon particles allows for excellent contact with hydrochloric acid and sodium tetrahydroborate solutions.

In Figure 1 (a–c) we have XRD patterns that are the average of NIST SRM 1649a and of the local urban and sub-urban dust samples. X-ray diffraction was performed using an incidence beam angle of 0.2° and 2θ scans with a 0.010° step and of 10 s duration. In these XRD patterns, there are characeristic peaks of the compounds. The NIST SRM 1649a (Figure 1a) contained quartz and gypsum, including other compounds at low proportions such as albite and microcline. The XRD patterns for both local dust samples (Figure 1b and Figure 1c) are very similar and showed quartz at a high proportion,

TABLE V
Elemental Analysis Expressed as % (N=4)

	NIST SRM 1649a Urban Dust	Local Suburban Dust Sample	Local Urban Dust Sample
% N	2.8 ± 0.02	0.25 ± 0.01	0.10 ± 0.01
% C	18 ± 0.01	5.14 ± 0.3	2.56 ± 0.03
% H	2.3 ± 0.05	0.97 ± 0.02	0.39 ± 0.02
% S	3.3 ± 0.03	0.08 ±0.002	0.18 ± 0.02

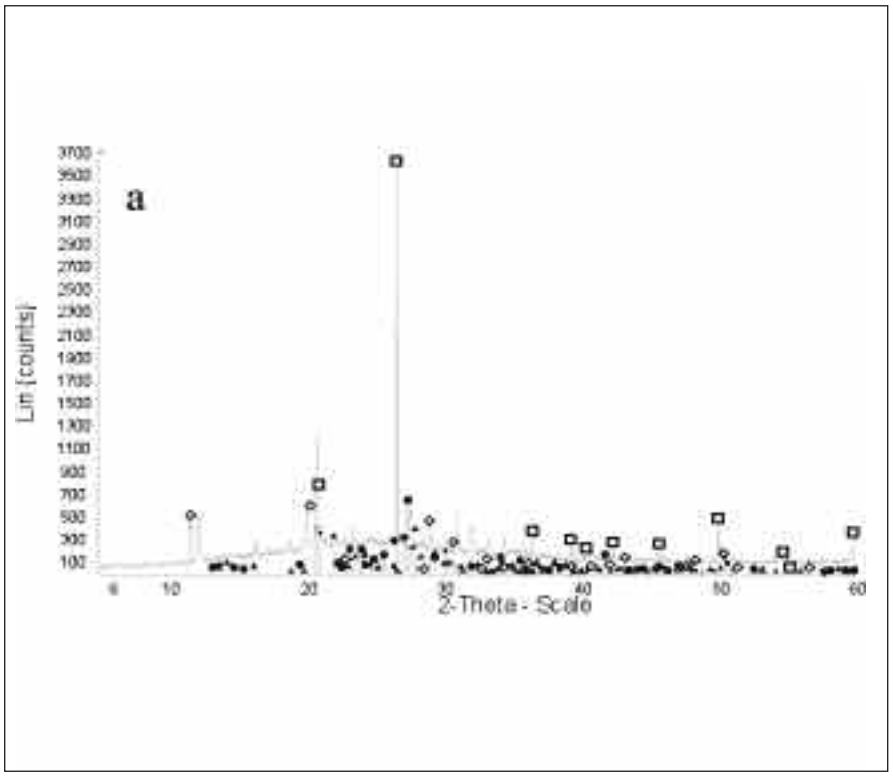

*Fig. 1 (a–c). X-ray diffraction (XRD) patterns of (a) NIST 1649a, (b) local urban dust sample, and (c) local sub-urban dust sample: Quartz (□), gypsum (▱), albite (▲), microcline (●), calcite (+), dolomite (x), orthoclase (Δ), and unknown peak (*).*

while albite, microcline, calcite, dolomite, and orthoclase are present at a low proportion. As is illustrated, these XRD patterns present several differences between the local dust samples and the NIST SRM 1649a sample. Firstly, gypsum was not identified in either of the local dust samples. Secondly, calcite and dolomite were not found in NIST SRM 1649a. Thirdly, both local dust samples showed two unknown peaks close to the highest quartz peak intensity. The differences in the chemical composition of the local urban and sub-urban dust samples could explain the low recoveries achieved when the aqueous slurries of these samples were analyzed.

In addition, differences in mean particle size were found. A Laser Coulter Series LS200 Fraunhofer optical model particle sizer with an LS-variable speed fluid module

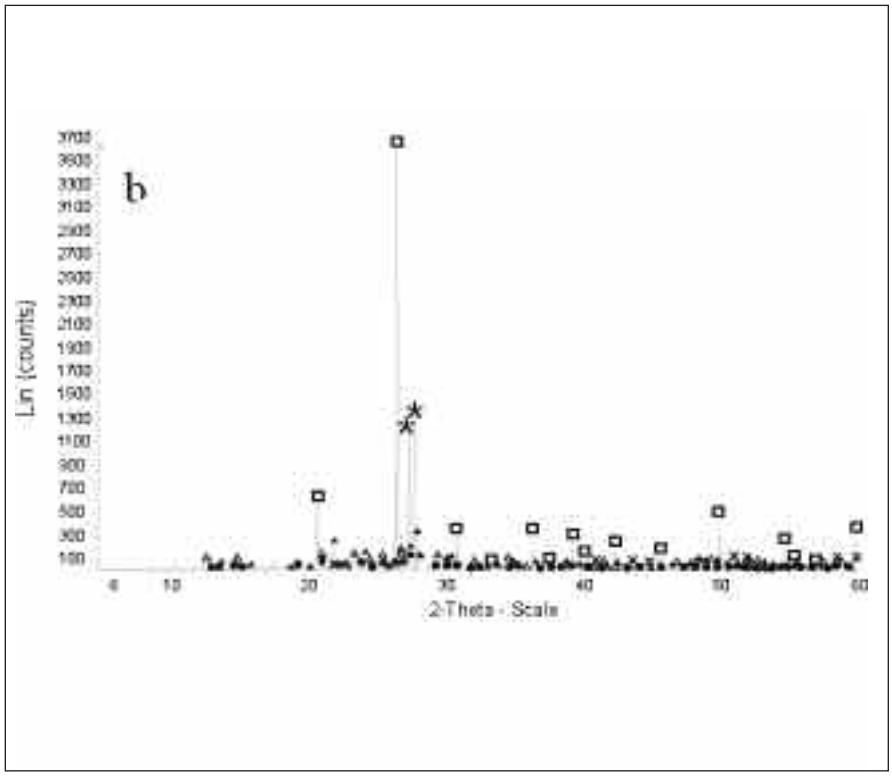

Fig. 1 (b). See previous page for caption.

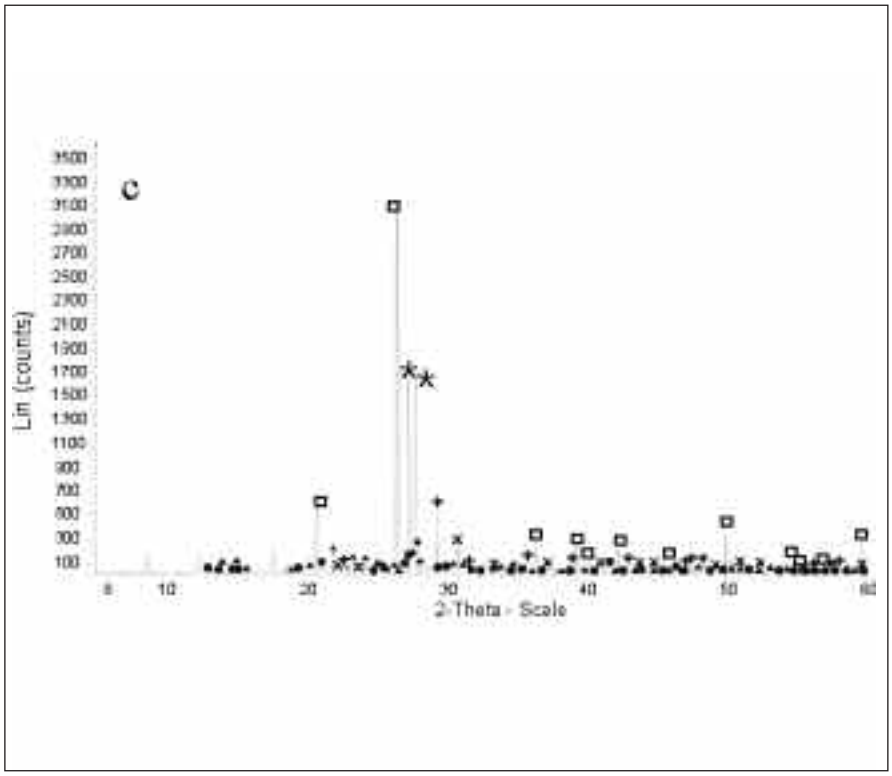

Fig. 1 (c). See previous page for caption.

(Coulter Electronics, Hialeah, FL, USA) was used to obtain particle-size distributions. The mean particle size of the NIST SRM 1649a is around 40 µm. The mean particle size of the local urban dust samples is around 180 µm. Mean particle size determines the hydride generation efficiency from aqueous slurries. Hydrochloric acid and sodium tetrahydroborate solutions cannot react with the analytes in the solid particles. Therefore, low hydride generation efficiencies were obtained from the metals trapped in the large solid particles of the local urban dust samples. On the other hand, there was good hydride generation efficiency for the NIST reference material because the sample consists of small particles (< 40 µm). Therefore, the trace elements As, Sb, and Sn could easily pass to the liquid phase and generate hydrides under conventional hydride generation conditions.

A study on the influence of particle size on hydride generation from aqueous urban dust slurries was carried out. Slurries were prepared by pulverizing a local dust sample in a vibrating ball mill. Different pulverization times (15 and 30 minutes) were investigated. From the pulverized samples, aqueous slurry samples were prepared. The mean particle size (measured by laser diffraction) and the As, Sb, and Sn concentrations corresponding to the two pulverization times were measured. The results showed that a pulverization time of 15 minutes is required to achieve a mean particle size lower than 40 µm. The recoveries for As, Sb, and Sn were 65, 50, and 85%, respectively, for the pulverized local urban dust slurries.

Acidified Slurries of NIST SRM 1649a and Local Urban Dust Samples

The values obtained using acidified slurries of NIST SRM 1649a (mean particle size 40 µm) and pulverized local urban dust samples (mean particle size 180 µm) were close to 100% for the target metals. The acid medium improves the mobilization of the analytes from the solid particles into the liquid media, which results in a significant improvement in the accuracy of the methods. When acidified slurries are used, the differences in chemical composition of the sample and mean particle size do not play an important role in the hydride generation efficiency. On the other hand, the recoveries achieved when using the acid liquid phase (obtained after acid slurry centrifugation) were lower (around 80%) than those obtained for acidified slurry samples. Thus, we can say that hydride generation occurs from the metal extracted into the acid solution and from the solid particle. As can be seen, the use of acids increases the hydride generation efficiency from solid particles. This procedure uses small volumes of acids at low concentrations (4.0 M) and can, therefore, be considered an environmentally friendly approach.

CONCLUSION

The acidified slurries of NIST SRM 1649a Urban Dust standard reference material and local urban dust samples allow the As, Sb, and Sn determination by hydride generation coupled to electrothermal atomic absorption spectrometry. Sample pre-treatment such as acid extraction is eliminated and the time required for pre-treating the samples is highly minimized. In addition, analyte loss and sample contamination is removed. Diluted nitric acid concentrations were used, even for acidified slurries, which implies an important reduction in waste. The overall procedure can be considered an environmental friendly process.

Chemical composition and mean particle size of the samples determine the accuracy of the results. For samples with a high mean particle size and low gypsum and low carbon content (in local urban dust samples around 180 µm), a pulverization sample step is required to achieve mean particle sizes lower than 40 µm. In addition, the use of acidified slurries is necessary to achieve accurate results. However, the use of aqueous slurries is enough to obtain accurate results for samples with a low particle size and high carbon content when As and Sn are determined.

ACKNOWLEDGEMENTS

This study was supported by Ministerio de Ciencia y Tecnología, project (REN2003-08603-C04-01). The authors thank Servicios Xerais de Apoio a Investigación (Universidad de A Coruña) for the technical support offered.

Received May 25, 2007.

REFERENCES

1. E. Merian, Metals and Their Compounds in the Environmental: Occurrance, Analysis and Biological Relevance, Weinheim VCH, Germany (1991).
2. European Community, Council Directive 2004/170/EC of 15 December 2004 relating to arsenic, cadmium, mercury, nickel and polycyclic aromatic hydrocarbons in ambient air. Off. J. L23, 3 (2004).
3. F. Fernández-Álvarez, M. Ternero-Rodríguez, A. J. Fernández-Espinosa, and A. Gutierrez-Daban, Anal. Chim. Acta 524, 33 (2004).
4. M. Sakata and K. Marumoto, Atmos. Environ. 36, 239 (2002).
5. P. E. Rasmussen, K. S. Subramanian, and B. J. Jessiman, Sci. Total Environ. 267, 125 (2001).
6. A. Chatterjee and R. N. Banerjee, Sci. Total Environ. 227, 175 (1999).
7. X. Feng, J. Y. Lu, D. C. Gregoire, Y. Hao, C. M. Banic, and W. H. Schroder, Anal. Bioanal. Chem. 380, 683 (2004).
8. V. Oliveira, J. L. Gómez-Ariza, and D. Sánchez-Rodas, Anal. Bioanal. Chem. 382, 335 (2005).
9. C. Moscoso-Pérez, J. Moreda-Piñeiro, P. López-Mahía, S. Muniategui-Lorenzo, E. Fernández-Fernández, and D. Prada-Rodríguez, Anal. Chim. Acta 526, 185 (2004).
10. M. M. Farinha, Z. Slejkovec, J. T. Elteren, H. Th. Wolterbeek, and M. C. Freitas, J. Atmos. Chem. 49, 343 (2004).
11. H. Matusiewicz, Appl. Spectrosc. Reviews 38, 263 (2003).
12. X. Querol, A. Alastuey, J. A. Puicercus, E. Mantilla, C. R. Ruíz, A. López-Soler, F. Plana, and R. Juan, Atmos. Environ., 32, 719 (1998).
13. J. Dêdina and D. L. Tsalev, Hydride Generation Atomic Absorption Spectrometry, Chichester, UK, pp. 155-157 (1995).

Antimony Determination in Mussel Samples by Atomic Absorption Spectrometry Using Palladium-Magnesium Nitrate as Chemical Modifier

B. Curros-Gontad, M.C. Barciela-Alonso, M.D. Buján-Villar, E. M. Peña-Vázquez, and *P. Bermejo-Barrera
Department of Analytical Chemistry, Nutrition and Bromatology, Faculty of Chemistry,
University of Santiago de Compostela,
Avenida das Ciencias s/n, Santiago de Compostela E-15782, Spain

ABSTRACT

A method for antimony determination in mussel tissue by ETAAS, using palladium-magnesium nitrate as a chemical modifier, was optimized. Before spectrometric analysis, the samples were mineralized by microwave heating using a mixture of nitric and sulfuric acid as the digesting agents. The optimum pyrolysis and atomization temperatures were 1100 and 1800 ºC, respectively. The method was precise (with %RSD <10%), accurate (with recoveries between 90–104%), and sensitive (LOD 0.02 μg g^{-1}). The method was applied to the determination of antimony in cultivated mussel samples from the Ría de Arousa, an estuary situated in Galicia (NW Spain).

INTRODUCTION

It has been demonstrated that antimony is a valuable tracer of anthropogenic impact on the environment (1). This element has low concentrations in the earth's crust (0.2–1.0 μg g^{-1}) and anthropogenic inputs may be easily evaluated. Up to 18,000 T Sb per year are estimated to enter the aquatic ecosystems. The occurrence of antimony pollution has been attributed to coal and fuel combustion, the production of alloys, and a large number of other industrial processes (manufacture of semiconductors, batteries, arms and bullets, cable sheathing, paints, flame retardants, chemicals, ceramics, etc.). Despite the clear impact of antimony on the environment, few studies have focused on measuring antimony in marine life (2).

The effects of heavy metals on marine life are very complex. These elements tend to concentrate in aquatic sediment and biota and are therefore present in the aquatic food chain, possibly also becoming a danger for human health. Shellfish, particularly mussels, accumulate metals from their aqueous environment, acting as pollution indicators. For this reason, it is absolutely necessary to set up a reliable analytical method for element determination in mussels (3). Moreover, antimony may be bound to organic compounds, and therefore a correct sample mineralization must be able to be carried out in order to obtain results with good precision and accuracy.

**Corresponding author.*
E-mail: pbermejo@usc.es

Nash et al. (4) wrote a critical review about methodologies for the determination of antimony in terrestrial environmental samples. Antimony determination in biological samples is often carried out using mixtures of oxidizing acids (sulfuric acid, nitric acid, perchloric acid) plus hydrogen peroxide to decompose matrices with high organic content, and using closed-vessel microwave (MW) heating to prevent Sb volatilization at high temperatures. Digestion prior to hydride generation coupled to inductively coupled plasma optical emission spectrometry (HG-ICP-OES) is commonly used (5–9) when analyzing biological materials, but inductively coupled plasma mass spectrometry (ICP-MS) (10–12) has less interferences and offers more sensitivity. Double-focusing ICP-MS was used to study antimony distribution patterns in the Mytillus edulis cytosols using size-exclusion chromatography as the separation technique (13). Recently, antimony was determined in biological samples using axial inductively coupled plasma time-of-flight mass spectrometry (ICP-TOFMS) with ultrasonic nebulization after flow injection (FI) on-line sorption/preconcentration in a knotted reactor (KR) with ammonium pyrrolidine-dithiocarbamate (APDC) as the complexant agent (14).

Hydride generation coupled to atomic absorption spectrometry (HGAAS) has been used to determine antimony in biological materials (15,16) and preconcentration of antimony hydride in a graphite furnace followed by atomization has been developed as another method to determine antimony (17,18). All these methods give low detection limits but have several drawbacks: ICP-based methods are expensive for routine analysis and hydride generation may not give 100% recovery when non-hydride-forming species are present in the sample, in addition to being a labor-intensive process. Electrothermal atomic absorption spectroscopy (ETAAS) is a widely used analytical tool for the determination of many trace metals in a wide variety of sample matrices. The sample matrix has a pronounced effect on the absorbance signal observed for a particular element. These effects often lead to systematic errors when determining metals in complex organic matrices and are the result of substances not fully volatilized prior to atomization of the metal. Therefore, optimization of the instrumental conditions is a

prerequisite for the development of an environmental analytical protocol using ETAAS. Koch et al. (19) carried out a simplex optimization of the instrumental conditions using a Placket–Burman method for the ETAAS determination of antimony in environmental samples. Tsalev et al. (20) studied the thermal stabilization of several volatile elements (including Sb) using mixed modifiers such as palladium-tungsten and Borba da Silva et al. (21) studied the influence of permanent modifiers (iridium and rhodium) in the antimony determination.

The purpose of this study was to determine antimony in digested mussel samples by electrothermal atomic absorption spectrometry using palladium-magnesium nitrate as the modifier. Moreover, antimony concentrations in mussels from the Ría of Arousa, one of the more productive aquaculture sites in Europe, are reported in this work.

EXPERIMENTAL

Instrumentation

A freeze-dry system from Labconco (Kansas City, MO, USA) was used to obtain lyophilized mussel samples. These samples were pulverized using a vibrating zircon ball mill (Retsch, Haan, Germany), equipped (with zircon cups (15 mL in size) and zircon beads (7 mm diameter).)

Sample digestion was performed using an Ethos Plus High Performance microwave station (Milestone, Bergamo, Italy).

Measurements were performed on a PerkinElmer® Model 1100B atomic absorption spectrometer, equipped with HGA®-700 graphite furnace atomizer, an AS-70 autosampler and deuterium background correction (PerkinElmer Life and Analytical Sciences, Shelton, CT, USA). The source of radiation was a hollow cathode lamp operating at 39 mA, with a spectral bandwidth of 0.2 nm and a wavelength of 217.6 nm. Pyrolytically coated graphite tubes with L´vov platforms were used. The total injected sample volume was 60 µL (2 injections of 30 µL). The graphite furnace program is listed in Table I.

Reagents and Standard Solutions

A stock standard solution of Sb (1000.065 µg mL^{-1}) was prepared by dissolving 0.2166 g of $K[Sb(OH)_6]$ (99.99%, Aldrich Chemical, Milwaukee, WI, USA) in ultrapure water and diluting to 100 mL.

69% nitric acid (TMA) and 96% sulfuric acid from Panreac SA (Barcelona, Spain) were used to perform the MW digestions.

Magnesium nitrate, Suprapur® (Merck, Darmstadt, Germany), was used to prepare the graphite furnace modifier. The palladium solution was prepared by dissolving 300 mg of palladium (99.999%) (Aldrich, Milwaukee, WI, USA) in 1 mL concentrated nitric acid and diluting to 100 mL with ultrapure water. If dissolution was incomplete, 10 µL of AnalR® 35% hydrochloric acid (BDH, Poole, UK) was added to the cold nitric acid. This solution was heated to gentle boiling in order to volatilize excess chloride.

Argon N50 (99.999% purity) was used as a sheath gas for the atomizer and to purge internally.

Ultrapure water, resistivity 18 MΩ cm, was obtained from a Milli-Q™ water purification system (Millipore, Bedford, MA, USA). All glassware was washed and kept in 10% (v/v) nitric acid for at least 48 hours, then rinsed three times with ultrapure water before use.

Procedure

Fresh cultivated mussel samples (*Mytillus galloprovincialis*) were collected at different sampling points from Ría de Arousa (Galicia, NW Spain) from mussel rafts (Figure 1). The samples were collected during four sampling periods (April 2002, July 2002, February 2003, and July 2003), 16 samples taken during each period. The samples were triturated, homogenized, and lyophilized. Afterwards, the samples were pulverized in a vibrating zircon ball mill for 30 minutes using 75% power and the samples placed into pre-cleaned polyethylene vials.

A 0.5-g portion of powdered sample was weighed into each digestion vessel and 1.5 mL of 69% HNO_3, 1 mL of 96% H_2SO_4, and 8 mL of water were added. Afterwards, the vessels were placed into the microwave oven. One sample vessel was pressure-controlled dur-

TABLE I
Graphite Furnace Temperature Program for Sb Determination[a]

Step	Temp.(ºC)	Ramp (s)	Hold (s)	Ar Flow (mL min^{-1})
Dry 1	120	5	40	300
Dry 2	150	5	30	300
Charring 1	480	15	40	300
Charring 2	1200	20	60	300
Atomization	1800	0	3	0 (read)
Clean	2400	5	10	300

[a] Injection of 30 mL → drying and charring steps → injection of 30 mL → full program.

ing the digestion operation. The temperature program used in the microwave oven lasted 25 minutes and consisted of 5 steps:
(a) 24 ºC, ramp 2 s;
(b) 90 ºC, ramp 2 s;
(c) 140 ºC, ramp 5 s;
(d) 200 ºC, ramp 5 s; and
(e) 200 ºC, hold 11 s.
The digested sample was adjusted to a final volume of 25 mL by addition of ultrapure water.

RESULTS AND DISCUSSION

Optimization of the Graphite Furnace Temperature Program

Experiments were carried out to determine the optimal temperatures and times for the drying, charring, and atomization steps using palladium-magnesium nitrate as the chemical modifier. The operating conditions were optimized considering maximum charring temperature, atomic peak shape, and atomic and background signals.

Two drying steps were used to eliminate water in the graphite tube: 120 ºC for 40 s, followed by 150 ºC for 30 s. For an efficient pyrolysis, two charring steps were used: the first at 480 ºC and the second at 1200 ºC. The introduction of these pyrolysis steps at 480 ºC reduce the background signal and improve the reproducibility of the results.

Determination of the optimal atomization temperature was carried out by studying the temperature ranging from 1500 ºC to 2200 ºC. We selected 1800 ºC as the optimal atomization temperature for the mussel digestion. Charring and atomization curves for a mussel digestion sample are shown in Figure 2.

The graphite tube was cleaned at 2400 ºC for 10 s using an argon flow of 300 mL min^{-1} in order to avoid memory effects.

Antimony preconcentration in the graphite tube was optimized by injecting 2 or 3 times 20 µL or 30 µL of sample and changing the digested sample volume (600 µL or 700 µL diluted to 1 mL). Drying and charring steps were performed between injections. Finally, two sample injections of 30 µL were carried out using 600 µL of digested sample diluted to 1 mL. Thus, a maximum absorbance signal was achieved and background absorption was minimized. The preconcentration program is shown in Figure 3.

The optimized temperature program for the antimony determination in digested mussel samples, using palladium-magnesium nitrate modifier as the chemical modifier, is listed in Table I.

Fig. 1. Sampling stations in the Ría de Arousa estuary.

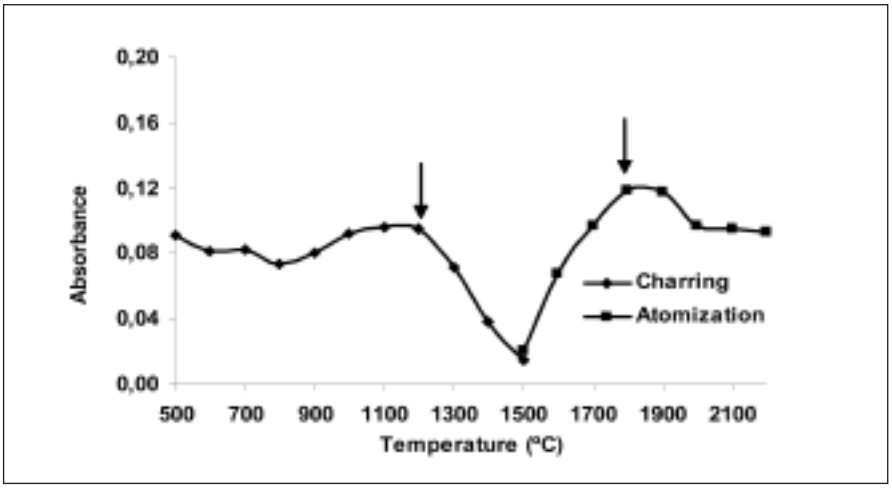

Fig. 2. Charring and atomization curves (optimal temperatures, 1200 and 1800 ºC).

Atomic Spectroscopy
Vol. 28(4), July/August 2007

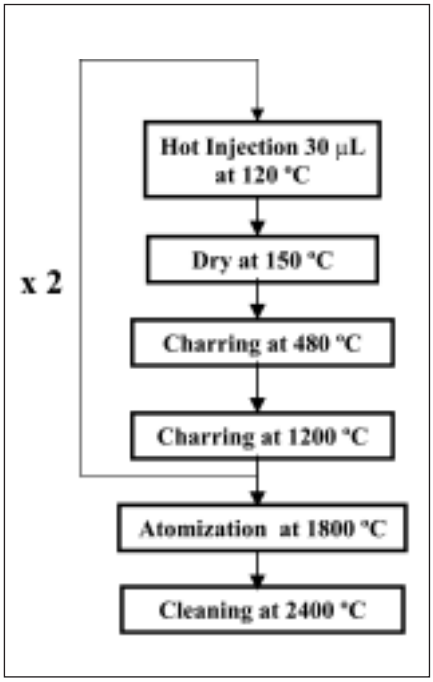

Fig. 3. Preconcentration program.

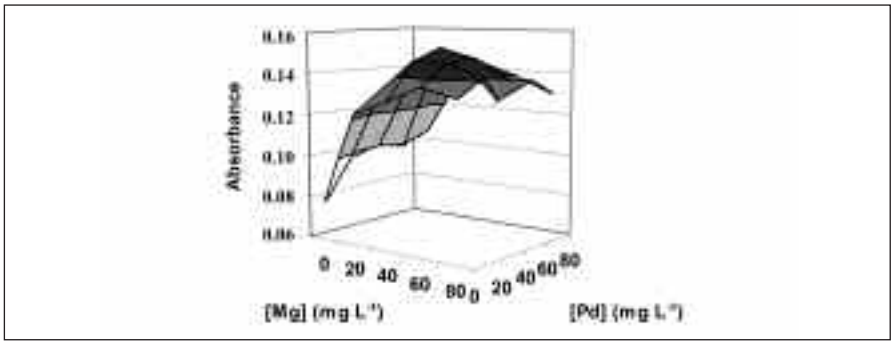

Fig. 4. Influence of palladium and magnesium nitrate concentrations in the absorbance of a sample digestion spiked with antimony solution.

Amount of Chemical Modifier

Experiments were carried out to determine optimal concentrations of both palladium and magnesium nitrate. The study was performed by spiking a mussel digestion with an aqueous antimony standard solution, then adding different concentrations of palladium and magnesium nitrate ranging between 0 and 80 mg L^{-1}. The absorbance values obtained are shown in Figure 4.

It can be observed that the highest absorbance signal is obtained when using 40 mg L^{-1} of magnesium nitrate and 40 mg L^{-1} of palladium. These modifier concentrations were selected for the following experiments.

Calibration and Standard Additions Graphs

In order to obtain a calibration graph, standard aqueous solutions containing antimony concentrations ranging from 0 to 10 µg L^{-1} were prepared. Appropriate volumes of palladium and magnesium nitrate solutions were added to provide concentrations of 40 mg L^{-1} for both modifiers. The standard additions method was used at a concentration range between 0–8 µg L^{-1} using a digested mussel sample (600 µL of mussel digestion diluted to 1 mL). The following equations were obtained:

Calibration graph:

$$QA = 0.0009 + 0.0105\ C$$
$$r = 0.9994$$

Standard addition graph:

$$QA = 0.0115 + 0.0127\ C$$
$$r = 0.9973$$

where QA is the integrated absorbance, C is the antimony concentration in µg L^{-1}, and r is the linear regression coefficient. Slopes of the calibration and addition graphs are not statistically comparable (a *t*-test was applied, 95% significance level) (22). Therefore, only the standard addition method can be used to quantify antimony in digested mussel samples.

Sensitivity

The limit of detection (LOD), the lowest concentration level that can be determined to be statistically different from a blank, is defined as LOD=3SD/m (where m is the slope of the addition graph), corresponding to a 99% confidence level. The limit of quantification (LOQ) is defined as the level above which quantitative results can be obtained with a specified degree of confidence. The recommended value is LOQ=10SD/m at the 99% confidence level. In both cases, SD is the within-run standard deviation of a single blank determination. The obtained values were 0.11 and 0.38 µg L^{-1} for the LOD and LOQ, respectively, based on 10 replicate determinations of the blank.

The LOD and LOQ for a mussel sample were 0.02 and 0.06 µg g^{-1}, respectively. These values were calculated using 0.5 g of lyophilized mussel sample, diluted to 25 mL and taking 600 µL to prepare the final solution with the modifier (1000 µL).

The characteristic mass, m_o, is defined as the mass of analyte in picograms required to give a signal of 0.0044 s for the integrated absorbance. The obtained characteristic mass was 23.1 ± 2.8 pg.

The method is sensitive enough to perform antimony determinations in most unpolluted shellfish samples.

Precision and Accuracy

The within-run precision of the method was calculated by analyzing 10 replicates of a digested mussel tissue sample. The obtained value for the relative standard deviation (%RSD) was 3.0% and includes variations due to instrumental and matrix factors.

The repeatability of the overall procedure based on five different digestions from the same mussel sample was 1.4% and this result is considered acceptable (<10%).

Accuracy was studied by using analytical recovery assays because a mussel reference standard material was not available. The recovery values were 90.3%, 104.2%, 93.7%, 96.9%, and 100.7% for 3, 5, 8, 10, and 15 μg L^{-1} of added antimony, respectively. Therefore, recovery was considered satisfactory.

Applications

The proposed method was applied to the determination of antimony in cultivated mussel samples (*Mytillus galloprovincialis*) from the Ría de Arousa, an estuary on the Galician coast (NW Spain). The treatment with nitric acid and sulfuric acid in high pressure bombs with microwave energy was applied and the resulting solutions were analyzed by graphite furnace AAS. Digestion was performed in duplicate for each sampling station, and the spectroscopic determinations were made in triplicate for each digest.

The samples were collected during four sampling periods (April 2002, July 2002, February 2003, and July 2003), 16 samples for each period. Only 14 samples had an antimony content above the detection limit and antimony was not detected in samples obtained in July 2002 and February 2003. The results for April 2002 and July 2003 are listed in Table II. Therefore it can be stated that the found concentrations are lower than the maximum antimony concentration allowed in food as specified by the U.S. Food and Drug Administration (2 μg g^{-1}) (23).

There is little literature published evaluating antimony concentrations in unpolluted mussels or in other kinds of seafood. Since mussels bioconcentrate metals in their tissues, they are considered pollution biomarkers. Zimmermann et al. reported that zebra mussels (*Dreissena polymorpha*) bioaccumulated antimony from road dust in laboratory exposure studies (12). Gagne et al. (24) reported that *Dreissena polymorpha* and *Elliption Complanata* (both freshwater mussels) accumulated antimony from a municipal effluent dispersion plume.

In an early study, Ikebe et al. (25) reported the antimony concentration in mussels to be 0.019 μg g^{-1}. Ferradelo et al. (13) determined a concentration of 0.075 ± 0.04 μg g^{-1} (wet tissue) in cytosol of *Mytilus edilus* mussels, where antimony was uniformly distributed between the fractions of different molecular weight ranging from less than 4 kDa to more than 30 kDa. Antimony concentration in river mussels (*Perna Viridis*) from the Pearl River Delta (South China) ranged from 0.09 to 0.76 mg g^{-1} on a dry weight basis (26).

The results of our study show that the antimony concentrations found in Ría de Arousa are similar or lower than those found in the currently available bibliography. The antimony concentration is low in mussels from Ría de Arousa probably due to the low concentrations of the element in seawater (0.15 μg L^{-1}) (27). These values are lower than in most estuaries (Tejo, Rhin, Tamar River, Tan Shui) and the open ocean (Atlantic Ocean) (0.2 μg L^{-1}) (2). This fact could be due to the pyritization of this element in the sediments, a phenomenon that happens in Arousa because of biodeposits generated from mussel aquaculture (28). However, the highest antimony concentrations appear in areas of the inner part of the Ría of Arousa, which could imply the anthropogenic origin of the element.

TABLE II
Antimony Content in Mussels from Ría of Arousa

Station No.	April 2002 Sb (μg g^{-1})	July 2003 Sb (μg g^{-1})
1	0.04 ± 0.01	ND
2	ND	ND
3	0.13 ± 0.01	--
4	0.04 ± 0.02	0.04 ± 0.01
5	0.12 ± 0.02	ND
6	0.15 ± 0.03	ND
7	0.15 ± 0.04	0.05 ± 0.01
8	--	ND
9	0.19 ± 0.03	0.04 ± 0.02
10	ND	0.04 ± 0.01
11	ND	ND
13	0.10 ± 0.02	ND
14	ND	ND
15	0.04 ± 0.03	ND
16	ND	0.08 ± 0.03
17	ND	ND

Results expressed as: average ± standard deviation (n =6).
ND : < 0.02 μg g^{-1}
– : Data not available.

CONCLUSION

This study developed a method for the direct determination of antimony in mussel tissue samples. The samples need very little pre-treatment, which reduces the possibilities of contamination. The use of palladium-magnesium nitrate as a chemical modifier was found to stabilize the analyte up to 1300 ºC.

The method shows acceptable precision (RSD <10%), sensitivity (LOD 0.02 μg g^{-1}), and accuracy (recoveries between 90–104%) in the determination of antimony in mussel samples from the Ria of Arousa, an estuary on the Spanish coast.

ACKNOWLEDGMENTS

This work was part of a project sponsored by the Spanish Government through the Ministry of Science and Education, Reference: REN2002-01941. E. M. Peña Vázquez acknowledges the financial support by the Galician Government (Xunta de Galicia) in the framework of the Isidro Parga Pondal program.

Received May 17, 2007.

REFERENCES

1. M.J. Cal Prieto, A. Carlosena, J.M. Andrade, M.L. Martínez, S. Muniategui, P. López-Mahía, and D. Prada, Water Air Soil Poll. 129(1-4), 333 (2001).
2. M. Filella and N. Belzile, Earth-Sci. Rev. 57, 125 (2002).
3. C. Locatelli, Food Add. Cont. 17(9), 769 (2000).
4. M.J. Nash, J. E. Maskall, and S.J. Hill, J. Environ. Monit. 2, 97 (2000).
5. B. Pahlavanpour, M. Thompson, and L. Thorne, Analyst 106, 467 (1981).
6. E. de Oliveira, J.W. McLaren, and S.S. Berman, Anal. Chem. 55, 2047 (1983).
7. P. Schramel and L.Q. Xu, Fresenius' J. Anal. Chem. 340, 41 (1991).
8. K.A. Anderson and B. Isaacs, J. AOAC Int. 78, 1055 (1995).
9. M.C. Jung, I. Thornton, and H.T. Chon, Sci. Total Environ. 295, 81 (2002).
10. M. Krachler, H. Radner, and K.J. Irgolic, Fresenius' J. Anal. Chem. 355, 120 (1996).
11. S. Wu, Y. Zhao, X. Feng, and A. Wittmeier, J. Anal. At. Spectrom. 12, 797 (1997).
12. S. Zimmerman, F. Alt, J. Messerschmidt, A. von Bohlen, H. Taraschewski, and B. Sures, Environ. Tox. Chem. 21(12), 2713 (2002)
13. C.N. Ferradello, M.R. Fernández de la Campa, C. Sariego-Muñiz, and A. Sanz-Medel, Analyst 125, 2223 (2000).
14. K. Benkhedda, H. Goenaga-Infante, E. Ivanova, and F.C. Adams, J. Anal. At. Spectrom. 15, 1349 (2005)
15. N. Ainsworth, J.A. Cooke, and M.S. Johnson, Environ. Pollut. 65, 65 (1990).
16. C. Rondon, J. L. Burguera, M. Burguera, M. R. Brunetto, M. Gallignani, and Y. Petit de Peña, Fresenius' J. Anal. Chem. 353, 133 (1995).
17. R.E. Sturgeon , S.N. Willie, and S.S. Berman, Anal. Chem. 57, 2311 (1985).
18. R. Kalähne, G. Henrion, A. Hulanicki, S. Garbos, and M. Walcerz, Spectrochim. Acta Part B 52, 1509 (1997).
19. I. Koch and C.F. Harrington, Talanta 44(5), 771 (1997).
20. D.L. Tsalev, V. I. Slaveykova, and R.B. Georgieva, Anal. Lett. 29(1), 73 (1996).
21. J.B. Borba da Silva, M. Bertília, O. Giacomelli, I. GonValves de Souza, and A.J. Curtius, Microchem. J. 60, 249 (1998).
22. R. Cela, Avances en Quimiometría Práctica, University of Santiago de Compostela, Spain (1994).
23. H. G. Seiler and H. Sigel, Handbook on Toxicity of Inorganic Compounds, Marcel Dekker, New York, USA, pg. 72 (1988).
24. F. Gagné, C. Blaise, I. Aoyama, R. Luo, C. Gagnon, Y. Couillard, P. Campbell, and M. Salazar, Environ. Toxicol. 17, 149 (2002).
25. K. Ikebe, R. Tanaka, and M. Ikeda, J. Food Hyg. Soc. Japan 24 (5), 480 (1983)
26. Z. Fang, Tox. Environ. Chem. 88(1), 45 (2006).
27. E. Peña Vázquez, J. Villanueva-Alonso, A. Bermejo-Barrera, and P. Bermejo-Barrera, J. Environ. Monit. 8, 641 (2006).
28 . S. Emigloru, D. Rey, and N. Petersen, Phys. Chem. Earth 29, 947 (2004).

Preconcentration of Nickel in Multi-walled Carbon Nanotubes Pretreated With Potassium Permanganate for Use as Solid-phase Extraction Adsorbent and Determination by Flame Atomic Absorption Spectrometry

***Qingxiang Zhou[a], Huahua Bai[a], and Junping Xiao[b]**

[a] School of Chemistry and Environmental Sciences, Henan Normal University, Henan Key Laboratory for Environmental pollution Control, Xinxiang 453007, P.R. China

[b] Department of Chemistry, University of Science and Technology Beijing, Beijing 100083, P.R. China

ABSTRACT

This paper presents a reliable method for the determination of nickel at trace levels in environmental samples with multi-walled carbon nanotubes (MWCNTs) used as a novel solid-phase adsorbent. Before use, the MWCNTs were oxidized with potassium permanganate under appropriate conditions. The factors that may affect the extraction efficiency of nickel were investigated, such as pH, the concentration and volume of elution, flow rate, volume of the sample solution, and interference of coexisting ions. The results showed good linearity in the concentration range of 1–100 ng mL^{-1} and a low detection limit of 0.60 ng mL^{-1}. This method was applied to the determination of nickel in real environmental water samples and excellent results were achieved. The MWCNTs exhibited high analytical potential for the preconcentration of nickel and the determination of trace nickel in samples such as environmental water, food, and wastewater from battery factories.

INTRODUCTION

It is well known that the release of heavy metals into the environment has gained great attention worldwide due to their toxicity and wide use. Nickel is a typical heavy metal that is used in electroplating, the synthesis of magnetic material, the manufacture of batteries, and as hydrogenation catalyst (1–4). For example, in the synthesis of carbon nanotubes through the method of chemical vapor deposition, nickel is used as metal catalyst particles (5). Because of the vast consumption of nickel-containing products, many nickel compounds enter into the environment which leads to an increase in environmental pollution. Nickel is ingested by humans through food and has even been detected in honey and baby foods (6–7). Excess exposure to nickel or nickel compounds can lead to abnormal function of the organs. For instance, nickel compounds can induce hypoxic stress in the lung cells and may lead to lung and nasal cancers (8-9).

Since the ingestion of an excess amount of nickel affects the normal function of the human body, it has become crucial to develop automatic, sensitive, fast, and accurate analytical methods to monitor this metal. Many methods are proposed in the literature (10–14) for the determination of trace nickel with merits such as high selectivity, sensitivity, and simple operation using electrochemistry, chromatographic, and spectrometric techniques. Inductively coupled plasma mass spectrometry (ICP-MS) is the best technique due to its low detection limits and multi-element determination capabilities (15–16). But these instruments are very expensive and are often not affordable for the general analytical laboratory. An atomic absorption spectrometer (AAS) is the most widely used apparatus because it is economical and offers speed, utility, and reliability. But the AAS method is not applied for the direct determination of nickel due to its low concentrations and matrix interferences in the analysis. Hence, a pretreatment / enrichment procedure is required to eliminate the interferences of coexisting substances and to enhance the sensitivity of the method.

The traditional pretreatment method of metal ions is liquid-liquid extraction, which uses different volatile organic compounds (VOCs). At present, alternative technologies have been established and the traditional liquid-liquid extraction method has gradually been substituted. Cloud point extraction is a frequently used method in which a small quantity of surfactant is employed as the extraction medium. For example, Giokas et al. (14) described a cloud point extraction combined with flow injection analysis using flame atomic absorption spectrometry (FAAS) to determine nickel in five real water samples with detection limits of 11 μg L^{-1}. Solid-phase extraction (SPE) is another technology often used for the pretreatment of nickel. Compared with the traditional pretreatment method, solid-phase extraction has many advantages such as simple operation, easy automation, low cost, requiring either little or no organic reagent, and results in high recoveries. As far as solid-phase extraction

**Corresponding author.*
E-mail: zhouqx@henannu.edu.cn
Tel: 86-373-3325971
Fax: 86-373-3326336

is concerned, the most important aspect is the adsorptive packing which is a key point that determines whether the developed method is excellent or not. From the literature published, it can be seen that many compounds have been explored as adsorbents for the enrichment of nickel, such as clay, 2-propylpiperidine-1-carbodithioate, chromosorb108, ambersorb-572, and Ni-ion imprinted polymer (17–21).

Recently, carbon nanotubes (CNTs), which are novel carbonaceous materials, have gained much attention. Many publications show that they can be applied widely due to their unique tubular structure (nanometer diameter), large length/diameter ratio, and can be used for special chemical and physical applications. For instance, CNTs are used as biosensors, modified electrodes, and so on (22–23). CNTs also possess high analytical potential as excellent adsorbent for solid-phase extraction due to their chemical stability and high specific surface area. Cai et al. (24–25) have explored the adsorptive ability of multi-walled carbon nanotubes to bisphenol A, 4-n-nonylphenol, 4-*tert*-octylphenol, and phthalate esters. The recoveries reported were 89.8–104.2% for bisphenol A, 4-n-nonylphenol, and 4-*tert*-octylphenol, and 80.3–104.5% for phthalate esters. Zhou et al. (26–27) applied MWCNTs as solid-phase adsorbent to concentrate nicosulfuron, thifensulfuron-methyl, metsulfuron-methyl, DDT and its metabolite, with favorable results. All results indicate that these materials quantitatively adsorb these organic contaminants. Simultaneously, much research was done on the performance of modified CNTs in order to expand their application in the analytical sciences and other fields based on adulteration and oxidation (28–29). Li et al. (29) compared the adsorptive capabilities of as-grown CNTs and oxidized CNTs by three different oxidants. The adsorptive capabilities to enrich cadmium were 1.1 mg g^{-1} for as-grown CNTs, 2.6 mg g^{-1} for H_2O_2, 5.1 mg g^{-1} for HNO_3, and 11.0 mg g^{-1} for KMnO4. The results indicate that potassium-permanganate-oxidized CNTs possess higher adsorptive capability than HNO_3 and H_2O_2 oxidized CNTs. The oxidized CNTs should have great potential for use as solid-phase adsorbents to heavy metals. To our knowledge, no literature has been published on the application of oxidizing CNTs with potassium permanganate for use as an adsorbent in order to concentrate trace nickel in environmental samples. In this study, the feasibility of oxidized CNTs with potassium permanganate as a solid-phase adsorbent to preconcentrate nickel was investigated.

EXPERIMENTAL

Instrumentation

A Model Z-5000 polarized Zeeman atomic absorption spectrophotometer was used (Hitachi, Ltd. Tokyo, Japan) fitted with a nickel hollow cathode lamp and equipped with Zeeman-effect background correction. The instrumental operating conditions are listed in Table I. A Model SHZ-3 (III) vacuum pump (Yuhua Instrument Co., Ltd., Zhengzhou, Henan, P.R. China) was used in the preconcentration process. An Agilent ZORBAX SPE C_{18} cartridge (Agilent Corporation, USA.) was modified for use as a microcolumn. A 0.2-g amount of oxidized MWCNTs was introduced into this microcolumn after wiping off C_{18}. Ultrapure water was obtained using a Model Ultra-Clear (S.G. Wasseraufbereitungsanlagen, Barsbüttel, Germany).

TABLE I
Operating Conditions of Flame Atomic Spectrometer

Parameters	
Lamp current	12 mA
Wavelength	232.0 nm
Slit	0.2 nm
Burner head	Standard type
Burner height	7.5 mm
Flame	Air-acetylene
Oxidant gas pressure	160 kpa
Fuel gas flow rate	2.2 L/min

Standard Solutions and Reagents

All reagents and chemicals used were of analytical grade. A stock standard solution (80 μg mL^{-1}) was obtained by dissolving nickelous chloride ($NiCl_2 \cdot 6H_2O$) in ultrapure water. Working standard solutions were obtained by appropriate dilution of the stock standard solution. The pH of the working solution was adjusted with diluents of nitric acid and ammonia.

Multi-walled carbon nanotubes with an average external diameter of 30–60 nm were kindly provided by Tsing-Nafine Nano-Powder Commercialization Engineering Center, Chemical Engineering Department of Tsinghua University (Beijing, P.R. China). The MWCNs used as the adsorbent were oxidized in a solution of potassium permanganate at 80 °C for 2.5 hours. Subsequently, they were washed with deionized water to remove remnant oxidant, dried at 100 °C for 2 hours, and then transferred to the microcolumn which had a frit at the bottom.

SPE Procedure

After the MWCNTs were introduced into the microcolumn, 50 mL of 1 mol L^{-1} HNO_3 and 50 mL ultrapure water were used for washing in order to remove the contaminants coming from the environment.

The procedure of the solid-phase extraction for Ni^{2+} ions was as follows: the MWCNTs were prewetted with 10 mL 1mol L^{-1} HNO_3 and 10 mL ultrapure water. Then,

the working solution containing 40 ng mL^{-1} of Ni^{2+} ions was passed through the microcolumn and the target analyte was adsorbed quantitatively on the MWCNTs. The analyte was desorbed with 5 mL of 0.5 mol L^{-1} HNO_3. Finally, the concentration of the analyte in the eluent was determined by FAAS.

Water Sample

In this experiment, four real water samples were used to evaluate the application of the established method. They were obtained as follows: Tap water collected from our laboratory, groundwater from Xinxiang, and water from the Gushan reservoir in Jiaozuo. The waste sample was collected from the preliminary wastewater sedimentation tank at Huangyu Electrical Appliance Industry Company. All water samples were immediately filtrated through 0.45-μm membranes and stored in brown glass containers. Then, the sample solution was passed through the microcolumn. After the target analyte was adsorbed quantitatively on the MWCNTs, the analyte was desorbed by 5 mL 0.5 mol L^{-1} HNO_3. Finally, the concentration of the analyte in the eluent was determined by FAAS.

RESULTS AND DISCUSSION

Optimization of pH on Adsorption

After oxidizing with potassium permanganate, the functional groups of a small quantity of carboxyl, lactones, and phenols were introduced onto the surface of the CNTs (29). It is known that the introduction of these subacid oxygen-containing groups onto the surface of carbon material increases the total acidity, and enhances the hydrophilic and ion-exchange capabilities (30). Therefore, the pH of the working solution sharply influences the ion-exchange capability of the CNTs and the electrostatic attraction between nickel as well as the negative charge on the surface of the CNTs.

In order to obtain a reasonable pH condition for enrichment, different pH values ranging from 2–10 of the working solutions were optimized. The results are shown in Figure 1. It is obvious that the recovery of Ni ion is less than 50% when the pH of the working solution is lower than pH 6. The recoveries obtained were over 80% when the pH value was larger than pH 6. When the pH of the working solution is lower than the isoelectric point, the charge will be neutralized which will decrease the adsorption capability to nickel. Li et al. (29) reported that the isoelectric point of as-grown is pH 5. However, we found that after oxidizing with potassium permanganate, the isoelectric point became lower than pH 5. When the pH of the working solution was 2 and 4, the recoveries of nickel were 30.5% and 43%, respectively, which is much lower than 82%, 81.5%, and 81.5% at pH 6, 8, and 10, respectively. Therefore, the pH of 6 was selected for further study.

Optimization of Eluent Concentration and Its Volume

An appropriate eluent should elute the target analyte efficiently and cause no interference in the determination of the analyte. Tuzen et al., Baytak and Türker, and Ersoz et al. (19–21) reported that with the SPE procedure, nitric acid was conventionally selected as the eluent for nickel. For this reason, in our experiment nitric acid was also selected as the eluent for the desorption procedure. Considering that different efficiency would be obtained when different concentrations of nitric acid were used, we tested five different concentrations to elute the retained cation from the adsorbent. The results in Figure 2 show that the recoveries of Ni^{2+}

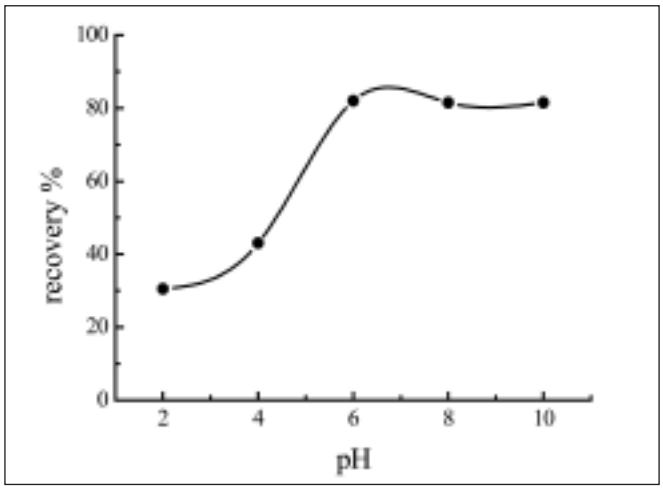

Fig. 1. Effect of pH on the adsorption of Ni^{2+} on MWCNTs Ni: 40 ng mL^{-1}

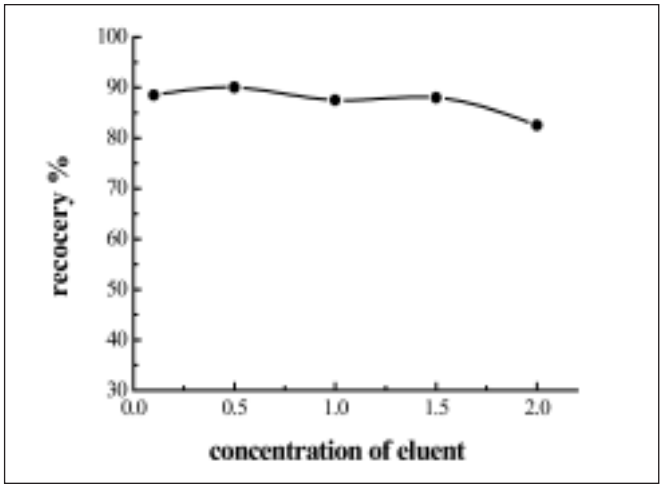

Fig. 2. Effect of eluent concentration on the adsorption of Ni^{2+} on MWCNTs Ni: 40 ng mL^{-1}

were obviously different, but 0.5 M HNO_3 was appreciably superior. Thus 0.5 M HNO_3 was selected for use in this study.

The volume of the eluent also affects the extraction efficiency. Thus, a series of experiments were designed to establish the most reasonable volume to maximize the enrichment factor without loss of extraction efficiency. The eluent volume was optimized between 4–8 mL. The results measured by FAAS are presented in Figure 3. It can be seen that when the eluent volume was 4 mL, quantitative recoveries were obtained; when the volume was up to 8 mL, there was no significant change. Finally, 5 mL was adopted to achieve the best enrichment performance as well as satisfying the injection volume required for FAAS analysis.

Optimization of Sample Flow Rate

The flow rate of the sample solution is an important parameter in most established methods, since it controls the time of the analysis and affects the retention of the target analyte on the microcolumn. The optimum flow rate was studied in the range of 1.54–3.77 mL min^{-1}. The results obtained in Figure 4 show that the recovery and the enrichment of nickel is not significantly affected by different sample flow rates. For all further studies, the maximal flow rate of 3.77 mL min^{-1} was selected in order to save analytical time.

Optimization of Sample Volume

In general, the main way to decrease the detection limit and increase the extraction efficiency is to increase the sample volume. This is an effective way to achieve satisfactory analytical performance. However, a limitless increase in sample volume would result in excess adsorptive capability of the adsorbent and not lead to the maximum enrichment factor. Thus, the sample volumes were optimized from 250 mL to 1500 mL with spiked concentrations of 40 ng mL^{-1} and all other enrichment conditions were kept constant in order to achieve an enrichment factor as high as possible. The results in Figure 5 show that the recoveries of nickel were in the range of 87.0–90.5% and there is no significant decrease when the volumes were up to 1500 mL. A volume of 250 mL was selected for further studies.

Effect of Coexisting Ions

In real environmental samples, the matrix is complicated and contains nickel and other ions, and the potassium-permanganate-oxidized MWCNTs are an appropriate adsorbent for nickel. Therefore, the influence of various co-existing compounds should be investigated. In this research, the spiked concentration of nickel was maintained at 40 ng mL^{-1}. A series of working solutions containing different ions at different concentrations were passed through the column at the optimum conditions adopted in the above experiments. The obtained recoveries of nickel and the tolerance limits of the co-existing ions defined as the largest amount making the recoveries of nickel less than 85% are listed in Table II. These results demonstrate that the presence of large amounts of co-existing ions have no obvious influence on the recovery of nickel.

Analytical Performance

Linear range, detection limit, and precision are important analytical performance parameters of the proposed method and were carried out at the optimum conditions adopted above. The obtained results listed in Table III demonstrate that there

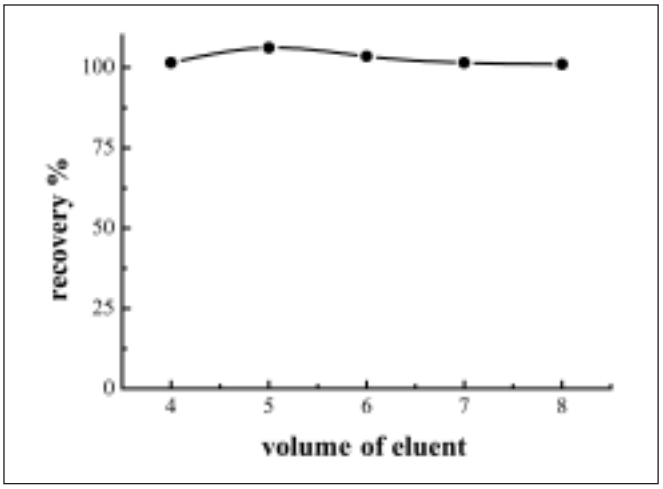

Fig. 3. Effect of eluent volume on the adsorption of Ni^{2+} on MWCNTs Ni: 40 ng mL^{-1}

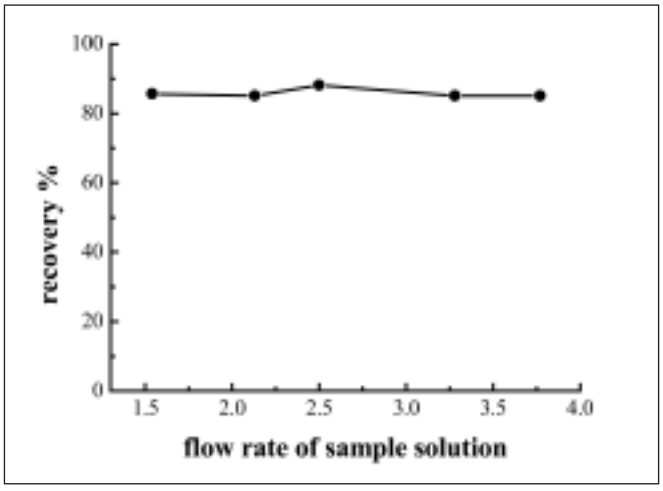

Fig. 4. Effect of flow rate of sample solution on the adsorption of Ni^{2+} on MWCNTs Ni: 40 ng mL^{-1}

was excellent linear correlation between ABS and the concentration of nickel in the working solutions ranging from 1 to 100 ng mL^{-1}. The correlation coefficient was 0.994. The detection limit was calculated based on the concentration corresponding to three times the standard deviation of 11 runs of the blank samples and the detection limit was 0.60 ng mL^{-1}. The precision of the proposed method was evaluated by calculating the relative standard deviation of six replicate working solutions containing 20 ng mL^{-1} nickel. The results of 2.82% show excellent precision.

Analytical Application

The results obtained in the determination of nickel in blank solutions of four real samples (tap water, groundwater, reservoir water, and wastewater) and their recovery measurements were used to evaluate the applicability and reliability of the proposed method. Table IV shows that nickel was only detected in the blank wastewater sample but not in any of the other blank solutions. The spiked recoveries (16 ng mL^{-1} of Ni^{2+} added) were investigated to validate the reliability of the proposed method. The extraction procedure of the spiked solutions was carried out as described above. The recoveries of nickel in the four samples are in the range of 84.2–121.1% (see Table IV).

CONCLUSION

A new method has been established using potassium-permanganate-oxidized MWCNTs as packing material for the solid-phase extraction of nickel from aqueous enviromental sample solutions. The method is simple, quick, and reliable. Under optimum conditions, the proposed method has a good linear range of 1–100 ng mL^{-1}, excellent reproducibility of 2.82%, and low detection limits of 0.60 ng mL^{-1}. The obtained recoveries of nickel in the four environmental water samples (tap water, groundwater, reservoir water, and wastewater) were in the range of 84.2–121.1%. These results demonstrate that MWCNTs oxidized with potassium permanganate have great potential

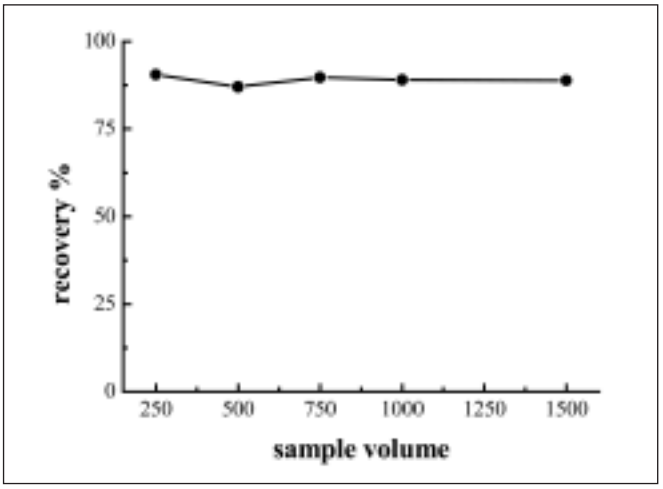

Fig. 5. Effect of sample volume on the adsorption of NI^{2+} on MWCNTs Ni: 40 ng mL^{-1}

TABLE II
Effect of Coexisting Ions (Ni^{2+}: 40 ng mL^{-1})

Co-existing Ions	Conc. of Co-existing Ions (µg mL^{-1})	Recovery of Nickel (%)
Na^+	200	104.5
K^+	200	98.5
Mg^{2+}	20	90.5
Ca^{2+}	20	99.0
Cu^{2+}	1	103.2
Al^{3+}	1	101.5
Fe^{3+}	1	85.8
SO_4^{2-}	200	104.5
Cl^-	200	98.5

TABLE III
Performance of Solid-phase Extraction of Nickel Under Optimum Conditions

Correlation Coefficient	**0.9994**
Linear range	1–100 ng mL^{-1}
Detection Limit	0.60 ng mL^{-1}
Enrichment Factor	50
Precision (20 ng mL^{-1}) (%RSD, N=11)	2.82%

TABLE IV
Determination of Ni^{2+} in Environmental Samples

Samples	Recovery (%)	
	Concentration	Added (16 ng mL^{-1})
Tap Water	–	86.7±3.1
Groundwater	–	84.2±3.2
Reservoir Water	–	92.9±5.2
Wastewater	8.3 ng mL^{-1}	121.1±1.4

– = Not found.

as an excellent adsorbent for the solid-phase extraction of nickel in environmental water samples and could be applied to monitoring nickel at trace levels in many fields.

ACKNOWLEDGMENT

This work was supported by High-Tech Research & Development Planning (863 Plan) of P.R. China (2006AA06Z424), the Natural Science Foundation of Henan Province (072300460010), the Personal Innovation Foundation of Universities in Henan Province ([2005]126), the Youth Science Foundation of Henan Normal University (2004005). The funds were obtained from the Henan Key Laboratory for environmental pollution control.

Received January 17, 2007.

REFERENCES

1. Z. Zhu, D. Zhu, N. Qu, and W. Lei, Mater. Des, In Press (2006).
2. H. Guo, Z. Qin, J. Wei, and C. Qin, Surf. Coating. Tech. 200, 2531,(2005).
3. X. He, W. Pu, H. Cheng, C. Jiang, and C. Wan, Energ. Convers. Manag. 47, 1879,(2006).
4. S. R. Kirumakki, B. G. Shpeizer, G. V. Sagar, K. V. R. Chary and A. Clearfield, J. Catal. 242, 319 (2006).
5. Th. D. Makris, L. Giorgi, R. Giorgi, N. Lis and E. Salernitano, Relat. Mater. 14, 815,(2005).
6. J. C. R. Garcia, J. B. Garcia, C. H. Latorre, S. G. Martín, and R. M. P. Crecente, J. Agric. Food Chem. 53, 6616 (2005).
7. P. Viñas, M. Pardo-Martínez and M. Hernández-Córdoba, J. Agric. Food. Chem. 48, 5789 (2000).
8. K. Salnikow, X. Li and M. Lippmann, Toxicol. Appl. Pharmacol. 196, 258 (2004).
9. M. Costa, T. L. Davidson, H. Chen, Q. Ke, P. Zhang, Y. Yan, C. Huang and T. Kluz, Mutat. Res. 592, 79 (2005).
10. A. Cobelo-García, J. Santos-Echeandía, R. Prego and O. Nieto, Electroanalysis. 17, 906 (2005).
11. G. Dugo, L. L. Pera, V. L. Turco, G. D. Bella and F. Salvo, J. Agric. Food. Chem. 52: 1928 (2004).
12. A. K. Singh, R. Singh, Journal of Inclusion Phenomena. 53, 249 (2005).
13. M. Frendikson, N. G. Carlsson, A. Almgren and A. S. Sandberg, J. Agric. Food. Chem. 50, 59 (2002)
14. D. L Giokas, E. K. Paleologos, S. M. Tzouwara-Karayanni and M. I. Karayannis, J. Anal. At. Spectrom. 16, 521 (2001).
15. L. Füchtjohann, N. Jakubowski, D. Gladtke, D. Klockowb and J. A. C. Broekaertd, J. Environ. Monit. 3, 681 (2001).
16. W. Hu, B. Hu and Z. Jiang, Anal. Chem. Acta. 572, 55 (2006).
17. M. Tuzen, E. Melek and M. Soylak, J. Hazard. Mater. 136, 597 (2006).
18. K. Suvardhan, K. S. Kumarc, D. Rekha, B. Jayaraj, G. K. Naidu, and P. Chiranjeevi, Talanta. 68, 735 (2006).
19. M. Tuzen, M. Soylak and L. Elci, Anal. Chim. Acta. 548, 101 (2005).
20. S. Baytak and A. R. Türker, J. Hazard. Mater. 129, 130 (2006).
21. A. Ersöz, R. Say and A. Denizli, Anal. Chim. Acta. 502, 91 (2004).
22. M. Yang, Y.Yang, Y. Liu, G. Shen and R. Yu, Biosens. Bioelectron. 21, 1125 (2006).
23. J. Wang, S. B. Hocevar and B. Ogorevc, Electrochem. Comm. 6, 176 (2004).
24. Y. Cai, G. Jiang, J. Liu and Q. Zhou, Anal. Chem. 75, 2517 (2003).
25. Y. Q. Cai, G. B. Jiang, J. F. Liu and Q. X. Zhou, Anal. Chem. Acta. 494, 149 (2003).
26. Q. Zhou, W. Wang and J. Xiao, Anal. Chem. Acta. 559, 200 (2006).
27. Q. Zhou, J. Xiao and W. Wang, J. Chromatogr. A. 1125, 152 (2006).
28. Y. H. Li, S. G. Wang, A. Y. Cao, D. Zhao, X. F. Zhang, C. L. Xu, Z. K. Luan, D. B. Ruan, J. Liang, D. H. Wu and B. Q. Wei, Chem. Phys. Lett. 350, 412 (2001).
29. Y. H. Li, S. G. Wang, Z. K. Luan, J. Ding, C. L. Xu, D. H. Wu, Carbon. 41, 1057 (2003).
30. J. W. Shim, S. J. Park and S. K. Ryu, Carbon. 39, 1635 (2001).

Books on the AAS, ICP-OES, ICP-MS Techniques

1. Concepts, Instrumentation and Techniques in Atomic Absorption Spectrophotometry

Authors: Richard D. Beaty and Jack D. Kerber
Order No. AA-914C (free of charge)
Ordering information: http://www.las.perkinelmer.com or contact your local PerkinElmer representative.

This book contains theoretical concepts and definitions of the science of atomic spectroscopy: atomic emission, atomic absorption, and atomic fluorescence. It also discusses high sensitivity sampling systems and the advantages and limitations of the cold vapor mercury, hydride generation, and graphite furnace atomic absorption techniques.
Also discussed are spectral and non-spectral interferences, including the goals and use of the stabilized temperature platform furnace (STPF) system.

2. Analytical Graphite Furnace AAS – A Laboratory Guide

Authors: G. Schlemmer and B. Radziuk
Order No. B051-1731
Ordering and price information: http://www.las.perkinelmer.com or contact your local PerkinElmer representative.

This book provides insight into the theoretical and practical aspect of graphite furnace AA making it the perfect reference resource for all laboratories wanting to use their graphite furnace more effectively.
Using an easy-to-follow style, the reader is guided from method development to calibration and validation of the instrument to the use of accessories and software in modern graphite furnace AA.

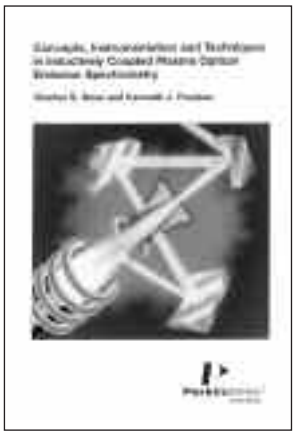

3. Concepts, Instrumentation and Techniques in Inductively Coupled Plasma Optical Emission Spectrometry

Authors: Charles B. Boss and Kenneth J. Fredeen
Order No. 005446B (free of charge)
Ordering information: http://www.las.perkinelmer.com or contact your local PerkinElmer representative.

This book presents the general characteristics of ICP-OES and ICP-OES instrumentation. It discusses ICP-OES methodologies including their application for the analysis of samples in the various industries such as agriculture and foods, biological and clinical, geological, environmental and water, metals, and organics.

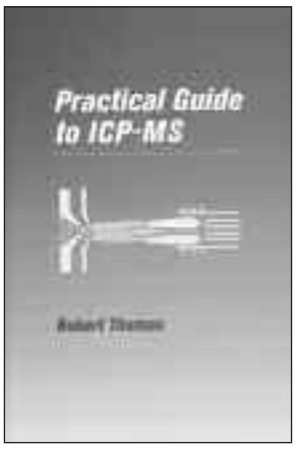

4. Practical Guide to ICP-MS

Author: Robert Thomas, Scientific Solutions (www. scientificsolutions1.com)
Published in 2004 by Marcel Dekker
Ordering and price information: http://www.crcpress.com/shopping_cart/products/product_detail.asp?sku=DK2933&parent_id=1151&pc=

The brand new reference book presents this powerful trace-element technique as a practical solution to real-world problems. The basic principles of ion formation/transportation/detection, common interferences, peak quantitation, sample preparation, contamination issues, routine maintenance and application strengths of ICP-MS are described in a way that is easy to understand for both experienced users and novices of the technique. In addition ICP-MS is compared with AA and ICP-OES in the areas of detection capability, dynamic range, sample throughput, ease of use and cost of ownership. The book concludes with an excellent chapter on the most important testing criteria when evaluating commercial instrumentation.

2008 Winter Conference on Plasma Spectrochemistry

TEMECULA, CALIFORNIA, USA, JANUARY 6–12, 2008

INFORMATION

For program, registration, hotel, and transportation details, visit the Conference website: http://www-unix.oit.umass.edu/~wc2006

OR contact: Ramon Barnes, ICP Information Newsletter, Inc., P.O. Box 666, Hadley, MA 01003-0666, USA

Tel: 413-256-08942, Fax: 413-256-3746, E-mail: wc2006@chem.umass.edu

The 15th biennial international Winter Conference will be held at the Pechanga Resort & Casino (www.pechanga.com) in Temecula, California, USA (www.temecula.org).

More than 600 scientists are expected and over 300 papers on modern plasma spectrochemistry will be presented. Six plenary lectures and 22 invited speakers will highlight critical topics in 12 symposia.

SYMPOSIUM FEATURES

- Elemental speciation and sample preparation
- Excitation mechanisms and plasma phenomena
- Flow injection and flow processing spectrochemical analysis
- Glow discharge atomic and mass spectrometry
- Inductively coupled plasma atomic and mass spectrometry
- Laser ablation and breakdown spectrometry
- Microwave atomic and mass spectrometry
- Plasma chromatographic detectors
- Plasma instrumentation, microplasmas, automation, and software innovations
- Sample introduction and transport phenomena
- Sample preparation, treatment, and automation; high-purity materials
- Spectrochemical chemometrics, expert systems, and software
- Spectroscopy standards and reference materials, databases
- Stable isotope analyses and applications

- Continuing Education Short Courses, Friday–Sunday, Jan. 4–6
- Manufacturer's Seminars, Friday–Sunday, Jan. 4–6
- Annual Golf Tournament, Sunday, Jan. 6
- Plasma Spectroscopy Instrumentation Exhibition, Tuesday–Thursday, Jan. 8–10
- Six Provocative Panel Discussions, Daily
- Workshop on New Plasma Instrumentation, Tuesday–Thursday, Jan. 8–10

Atomic Spectroscopy
Vol. 28(4), July/August 2007

PerkinElmer Life and Analytical Sciences
710 Bridgeport Avenue
Shelton, CT 06484-4794 USA
Phone: (800) 762-4000 or
(+1) 203-925-4602
www.perkinelmer.com

007821_04

PerkinElmer®
precisely.